SINTEF

Parametric design to minimize the embodied GHG emissions in a ZEB.

Lobaccaro, G., Wiberg, A. H., Ceci, G., Manni, M., Lolli, N., & Berardi, U.

1   Parametric design to minimize the embodied GHG emissions in a ZEB

2   Gabriele Lobaccaro[a*], Aoife Houlihan Wiberg[a], Giulia Ceci[b], Mattia Manni[b,c], Nicola Lolli[d], Umberto Berardi[e]

3   [a] *Department of Architecture and Technology, Faculty of Architecture and Design, Norwegian University of Science and Technology NTNU,*

4   *Trondheim, Norway.*

5   [b] *Faculty of Architectural Engineering, Department of Civil and Environmental Engineering, University of Perugia Perugia, Italy.*

6   [c] *CIRIAF – Interuniversity Research Center on Pollution and Environment "Mauro Felli", Department of Engineering, University of Perugia,*

7   *Perugia, Italy.*

8   [d] *SINTEF – Building and Infrastructure, Architecture, Materials and Structures, Trondheim, Norway.*

9   [e] *Ryerson University, Department of Architectural Science, Toronto, Canada.*

10   [*]*Corresponding author. Tel.: +47 918 13 568. E-mail address: gabriele.lobaccaro@ntnu.no (G. Lobaccaro).*

11   **Abstract**

12   This work aims to apply parametric design in order to minimize the embodied greenhouse gas emissions and operational energy in a zero emission building in Oslo, Norway. An original generative workflow based on parametric design was developed in the *Grasshopper* environment to conduct energy analyses such as solar radiation and daylighting, and environmental impact analysis, in order to evaluate the embodied and operational greenhouse gas emissions of the building. The workflow was generated in order to parametrically control several building features while varying the building shape, the dimensions of construction components and the quantity of materials. The process leads to the generation of shapes with the least environmental impact. The workflow allows the modification of the initial shape of the *Base Case* by running iterative simulations through the *Galapagos* and *Octopus* evolutionary solvers. For each stage of the shape's optimization, through passive and active strategies, the embodied emissions and energy balances were estimated in order to evaluate how the building design would vary in terms of energy and environmental impact and to identify the implications for the design. This paper shows how design options with low levels of embodied emissions can be generated and optimized automatically, and also demonstrates how a parametric design approach provides the designer with suggestions of low-impact solutions, which can then be integrated and considered early in, and throughout, the design process in a holistic manner.

27   **Keywords:** *Zero Emissions Building; Parametric design; Evolutionary computing; Embodied emissions; Life Cycle Assessment*

29   1. Introduction

30   The environmental impact of buildings on global energy demands and on greenhouse gas (GHG) emissions released to the atmosphere has rapidly increased during recent decades. Over 40% of global energy consumption and about 18% of GHG emissions are contributed by the building sector [1]. The current regulations to reduce energy consumption, and thereby GHG emissions, from buildings have focused on the operational phase [2, 3, 4].

35   An intensive focus on lowering the operational energy consumption in buildings during the past decade has emerged. From next year, all new public buildings in Europe will have to be near-zero energy [2, 3]. However,

current legislation excludes the assessment and reduction of the embodied energy and the embodied GHG of buildings.

The embodied energy and GHG emissions differ depending on the building design, the energy intensity of its materials, the national energy mix and the quantity of materials used [5, 6]. This is in line with the consensus reached in the International Energy Agency (IEA) Annex 57, 'Evaluation of embodied energy & CO_2 equivalent emissions for building construction', where the focus is on reducing environmental impacts from operational energy use needs, with a parallel emphasis on reducing environmental impacts embodied in the building materials and components [7].

Methodological improvements have been made in recent years in developing and harmonizing the life cycle assessment (LCA) method for buildings, including international standards such as ISO 21929 [8], ISO 21931 [9] and the European standards developed by Technical Committee TC350, including EN 15643 [10] and EN 15978 [11]. In these standards, environmental product declarations (EPD) of construction materials, which utilize a process based on LCA methods, are seen as a source of information (i.e. ISO 21930:2007 and EN 15804:2012+A1:2013, both currently under revision) for GHG emissions calculation in buildings.

1.1. *ZEB as solutions for GHG emissions reduction*

In response to the recast EPBD (Directive 2010/31/EU) [2] and, more recently, of the Energy Roadmap 2050 [12], the concepts of net zero energy buildings and zero emission buildings (ZEB) were realized to address and meet the challenges of reducing energy consumption and producing energy from renewable sources in order to reduce GHG emissions. A net zero energy building is defined as a building with high energy efficiency and enough on-site renewable energy generation to cover its energy consumption on an annual basis. In this respect, relevant contributions are included in a review and classification of definitions [13, 14, 15], such as the work done in the framework of the IEA 'Solar Heating and Cooling (SHC) Task 40 Net Zero Energy Solar Buildings', in which an updated state-of-the-art on zero energy buildings and their classifications have been provided based on a study of 30 net zero energy buildings worldwide, which were analyzed and monitored for at least 12 months in order to define best practice and to develop design and energy guidelines [16, 17, 18, 19, 20]. Other studies include more detailed definitions, for example in Marszal et al. [21], an overview of existing net zero energy definitions is provided, while Sartori, Napolitano, and Voss [22] propose a consistent framework in their definitions work.

Methodologies for calculating the performance of ZEB buildings are described in Marszal et al. [21]. In particular, some existing definitions explicitly integrate elements of LCA, as seen in [23] and [24]. The work conducted by Torcellini et al. [14] proposed a categorization of zero energy buildings into four clusters based on boundary conditions, performance and metrics. Among these, some net zero energy emissions buildings are identified—capable of producing at least as much in situ emissions-free energy as is required to meet their operational energy use demands. In Lund et al. [25], the zero energy and zero emissions buildings are grouped according to energy demand and installed systems for energy production.

During the past few decades, the use of LCA to evaluate the environmental impact of materials is becoming increasingly common. Life cycle assessment is a method for evaluating potential environmental impacts and resources used throughout a product or system's life cycle [26]. The standard EN 15978:2011 [11] divides the life cycle stages of a building into the following stages: product stage, construction stage, operational stage and the end-of-life stage. This method was demonstrated and applied in several studies in literature [23, 27, 28, 29,

30, 31, 32, 33]. There is considerable evidence to show that current calculation approaches, methods, indicators and data still continue to vary greatly across the world [34, 35, 36, 37, 27, 38]. For example, the results of a detailed comparative analysis of over 80 international case studies show a high variability (up to 100 times) of embodied GHG emissions due to methodological differences employed in the LCA. These differences include the LCA method used, the system boundaries, the assumed future scenarios for the service life of materials and end-of-life treatments, the reference study period, and the source of data, as described in [5].

LCA results are found to be inconsistent and vary according to the settings, approaches and findings—which differ from country to country [5, 39]. Furthermore, the study by Säynäjoki et al. [34] corroborates the high divergence in results from 116 cases from 47 scientific articles which were analyzed to find out whether these differences can be explained by contextual differences or methodological choices. It was concluded that subjective choices in all the major LCA phases are so significant that they do not offer reliable enough background information for policy-making without a deep understanding of the basis of a certain study, as well as a good methodological knowledge. In addition, incomplete reporting of methodological detail and the parameters of LCAs makes it challenging for experts in the field; there is also a lack of explanation for the variance in the LCA studies reviewed. In addition, Birgisdottir et al. [5] found a large variation in the life cycle included in the LCA of the different case studies, which also correlates well with the findings of Pomponi and Moncaster [37]. One of the key findings of Georges et al. [27], is the significant influence of the different scenarios for $CO_{2\text{-eq}}$ factors of the electricity supply on the performance of ZEB buildings. In particular, the introduction of a 'symmetric' emission factor, which means that the same $CO_{2\text{-eq}}/kWh$ factor for both export and import of electricity has been used.

The study here presented aims to propose a new approach for the investigation of the variation of the embodied and operational GHG emissions due to the different building's input parameters (e.g. materials, technologies, components, etc.) and dimensions (e.g. shapes, positions and size of the windows, etc.) for optimizing the design of a ZEB located in Oslo (Norway). The approach is focused on multi-objective optimization of passive and active strategies, as well as the assessment of embodied and operational emissions throughout the design process.

1.2. *The ZEB and LCA framework in Norway*

In Europe, the assessment of sustainable buildings throughout their whole life cycle is not regulated by any policy measures. The Norwegian government introduced the concept of low-energy buildings through the technical regulations of Norwegian Standards NS3700 [40] and NS3701 [41].

In addition, a Norwegian ZEB definition, including the different ambition levels, was introduced in [42, 43, 44]. According to Dokka et al., the Norwegian ZEB focuses on GHG emissions rather than energy; therefore, their performance indicator is measured in $kgCO_{2\text{-eq}}$ [42]. The ambition levels of ZEB are based on the LCA system boundaries defined in EN 15978 [11] and described in [42, 43, 44] (as shown in Table 1). The lowest level, ZEB–O–EQ, indicates a building characterized by an emission level of zero for operation (O), excluding the energy required for appliances and equipment (EQ). The ZEB–COM class also includes construction (C), operation (O) and the embodied emissions of a building's materials (M). Finally, the ZEB–COMPLETE level takes into account all the previous stages, as well as the demolition and recycling phases.

Previous publications have already reported on the performance of the first-stage Norwegian ZEB residential concept model [27, 45, 46]. The goal was to create a theoretical concept model for a single-family ZEB, based

1   on technologies and materials currently available in the market today. As described in [45, 46, 47], the results

2   show that the concept model is able to counterbalance emissions from operation energy use, ZEB–O. However,

3   it is unable to counterbalance the embodied emissions from materials in additional to operational energy use,

4   ZEB–OM. Therefore, the approach developed in this paper aims to reach the level of ZEB–OM by creating a

5   workflow based on parametric design principles that is able to maximize the energy production from active solar

6   systems and minimize the embodied emissions and operational energy demand.

7   Table 1. ZEB classification [42, 43, 44] according to the building life cycle phases [11].

Levels of ZEB	Product stage			Construction process stage		Use stage								End-of-life				Benefits and loads beyond the system boundaries			
	A1	A2	A3	A4	A5	B1	B2	B3	B4	B5	B6	B6	B7	C1	C2	C3	C4	D1	D2	D3	D4
	Raw material supply	Transport	Manufacturing	Transport	Construction installation process	Use	Maintenance	Repair	Replacement	Refurbishment	Operational energy use (space heating)	Operational energy use (appliances)	Operational water use	Deconstruction demolition	Transport	Water processing	Disposal	Reuse	Recovery	Recycling	Exported energy / potential
ZEB–O–EQ	−			−				−			−	✓	−	−			−			−	−
ZEB–O			−					−			✓	✓	−	−			−			−	−
ZEB–OM	✓				−			−			✓	✓	−	−			−			−	−
ZEB–COM	✓				✓			−			✓	✓	−	−			−			−	−
ZEB–COME	✓				✓			−			✓	✓	−	✓			−			−	−
ZEB–COMPLETE	✓				✓			−			✓	✓	−	✓			−			✓	−

8   *O (operation), EQ (appliances and equipment), M (material), C (construction)

9   The symbol ✓ indicates the boundary conditions used to achieve the different levels of ZEB.

10   2. **Parametric approach to emissions calculation in ZEB**

11   Parametric design principles describe a parameter-driven approach to the design process in which everything

12   that can be designed is represented by parameters. In this study, this approach mainly focuses on the definition of

13   a workflow that enables generation of an optimized building's shape throughout a form-finding process by

14   varying the building's input parameters and dimensions throughout the various stages of the design process. The

15   approach starts from the formation of a building concept and finishes with the definition of building form, with

16   parametric optimization of the building's features and components [48]. The advantages of a parameter-driven

17   approach are well-documented in literature [49]. It enables a multi-objective optimization processes that can

18   define optimized building shape configurations by testing different solutions, simultaneously and automatically,

19   without having to manually build the design detail of the building model each time that one of more parameters

20   are modified. At building scale, the parameters that may enable the optimization of the building's shape could

21   include, among others, the building features' dimensions and peculiarities (e.g. volume, height, width, length,

22   orientation, etc.), the building's construction elements (e.g. window dimensions and positions, inclination of

23   roof, exposure of the façades, etc.) and the building's energy (i.e. energy consumption, energy demand and

24   production) and environmental impact (e.g. quantity of materials, embodied emission, operational energy) The

25   workflow defined in this study has taken into account all of these aspects and has applied them to a case study

building in order to control and optimize (parametrically) its shape, energy performance and environmental impact. Similar approaches have been adopted in other studies. For example, the research conducted by Yun Kyu [50] proposed a method to represent geometry by implementing agent points (nodes) showing a novel solution for form-making. The results demonstrated how the proposed workflow enables more-efficient buildings, with a higher amount of solar radiation caught by the building envelope. A similar approach has been developed by Lobaccaro et al. [51]. By contrast, the study carried out by Zani [52] describes a generative algorithm for handling variable hypotheses on user occupancy that can influence building energy performance (Table 2).

Recently, the use of parametric tools has also been adopted for the calculation of a number of other performance aspects other than solar radiation, such as emissions from operational energy and embodied GHG emissions from materials. It should be noted that the system boundary considered in the LCA will differ based on the tools used and the purpose of the study in which the tool is applied. Many tools performing parametric analyses on the aforementioned performance aspects already exist on the market but none exist that dynamically link robust and reliable ZEB emissions data with other data in relation to energy or the interoperability with other digital environments, such as the Revit BIM model. In particular, some studies led to the development of new methodologies that enable the integration of two or more energy and/or environmental assessments [53, 54, 55] (Table 2). Nevertheless, it become increasingly necessary to develop a parameter-driven approach to conduct fast and simplified LCA analyses during the early stage of the design process by integrating "calculation sheets" (e.g. Excel or online databases) with 3D modeling software such as *Rhinoceros* or *Revit*. In this regard, Kokkos [56] developed a set of components for *Grasshopper* that enable LCA analysis of an industrial steel-framed pavilion, while visualizing the geometry variations in real time. The research conducted by Hollberg [57] achieved similar results and extended the algorithm to all the building's components, not just the frame. Even with the introduction of an evolutionary solver for the optimization of the building's shape, it did not enable free control: only minimal control was possible through a few parameters, such as the number of levels and the building footprint. In this regard, an overview of important recent studies is provided in Table 2. From the analysis of the existing workflows, it was revealed that none of them allow the simultaneous optimization of (i) embodied emissions (ii) solar radiation (iii) daylighting and (iv) buildings shape.

Therefore, based on this gap in existing literature concerning the workflows for LCA calculation and multi-objective optimization, the purpose of this work is to develop a workflow that enable the concurrent optimization of all these aspects.

Table 2. Overview of the existing workflows for LCA calculation and multi-objective optimization.

Authors	Reference	Year	Location	Case study	Input*					Tools	Output**				Visualization	
					Wd	Gd	Mp	En	Lce		Ee	Oe	Irr	Df	3D	Graphs
Azzouz et al.	[58]	2017	UK	Office building	✓	✓	✓	✓	✓	IMPACT	✓	✓	—	—	—	—
Ylmén et al.	[59]	2017	Sweden	Apartment	✓	✓	✓	✓	✓	EnergyPlus; Heat 3; Therm	✓	✓	—	—	—	✓
Ramin et al.	[60]	2017	Iran	Generic envelope	✓	✓	✓	✓	✓	N/A	✓	✓	—	—	—	✓
Braulio-Gonzalo et al.	[61]	2017	Spain	Generic envelope	✓	✓	✓	✓	✓	HULC	✓	✓	—	—	—	✓
Pomponi et al.	[62]	2017	UK	Generic envelope	✓	✓	✓	✓	✓	MATLAB; OpenLCA	✓	✓	—	—	—	✓
Lolli et al.	[53]	2017	Norway	ZEB residential single-family house	✓	✓	✓	✓	✓	Excel	✓	✓	—	—	—	✓
Tuncer	[54]	2017	Norway	ZEB residential single-family house	✓	✓	✓	✓	—	Flux.io; Revit BIM; Dynamo; ZEB Excel tool; EPD data	✓	—	—	—	✓	✓
Slånke and Auckland	[55]	2017	Norway	ZEB Living Lab to ZEN	✓	✓	✓	✓	—	Flux; Revit BIM; Dynamo; ZEB Excel tool	✓	—	—	—	✓	✓
Zani et al.	[52]	2017	Italy	University campus	✓	✓	✓	✓	—	Sketchup; Rhinoceros; Grasshopper; Ladybug; Honeybee; EnergyPlus; Octopus	—	✓	✓	—	✓	—
Bonomo et al.	[63]	2017	Undefined	Building Integrated Photovoltaic (BIPV) façade	—	✓	✓	✓	—	Excel	—	—	—	—	—	✓
Lobaccaro et al.	[51]	2016	Trondheim	Row houses	✓	✓	—	—	—	Rhinoceros; Grasshopper	✓	✓	✓	—	✓	—
Hollberg et al.	[57]	2016	Germany	Single-family house	✓	✓	✓	✓	✓	Rhinoceros; Grasshopper	✓	✓	—	—	✓	✓
Ashouri et al.	[64]	2016	Undefined	Generic envelope	✓	✓	✓	✓	✓	MATLAB	✓	✓	—	—	—	✓
Azari et al.	[65]	2016	USA	Office building	✓	✓	✓	✓	✓	Athena Impact Estimator; ANN	✓	✓	—	—	—	✓
Kokkos	[56]	2015	Netherland	Industrial pavilion	—	✓			✓	Rhinoceros; Grasshopper; Octopus	✓		—	—	✓	—
Yun Kyu et al.	[50]	2009	USA	Single-family house	✓	✓	✓	✓	—	Excel	—	✓	✓	—	✓	—
Luisa Caldas et al.	[66]	2001	USA	Office building	✓	✓	✓	✓	—	N/A	—	—	✓	✓	—	✓
Proposed workflow		2017	Norway	Single-family house	✓	✓	✓	✓	✓	Rhinoceros; Grasshopper; DIVA for Gh; Ladybug; EnergyPlus; Octopus	✓	✓	✓	✓	✓	✓

1 *The input values are: weather data (Wd), geometric dimensions (Gd), material properties (Mp), energy standards (En), life cycle emissions (Lce).
2 **The output values are: embodied emission (Ee), operational energy (Oe), solar irradiation (Irr), daylight factor (Df).

3. **Methodology**

The aim of this work is in line with one of the key questions identified as further work in the IEA Annex 57: 'What are the possibilities for new calculation methods and 3D models that can better consider embodied impacts both early on and throughout the design process' [7]. In order to address this question, the work presented in this paper has focused on developing an original parameter-driven approach based on an integrated design principles workflow applied to a ZEB concept model, herein referred to as the *Base Case*. The workflow enables energy analysis by studying factors such as solar radiation (Irr_{gl}) and daylight factor (Df), as well as environmental impact analysis, such as LCA analyses, by evaluating embodied emissions (Ee) and operational emissions (Oe). In Figure 1, the flowchart (described in detail in the following sections) shows the workflow, indicating the input data used and analyses conducted, using specific tools at each stage of the design process. The process leads to the continuous generation of optimized building shapes with minimized energy use and environmental impact.
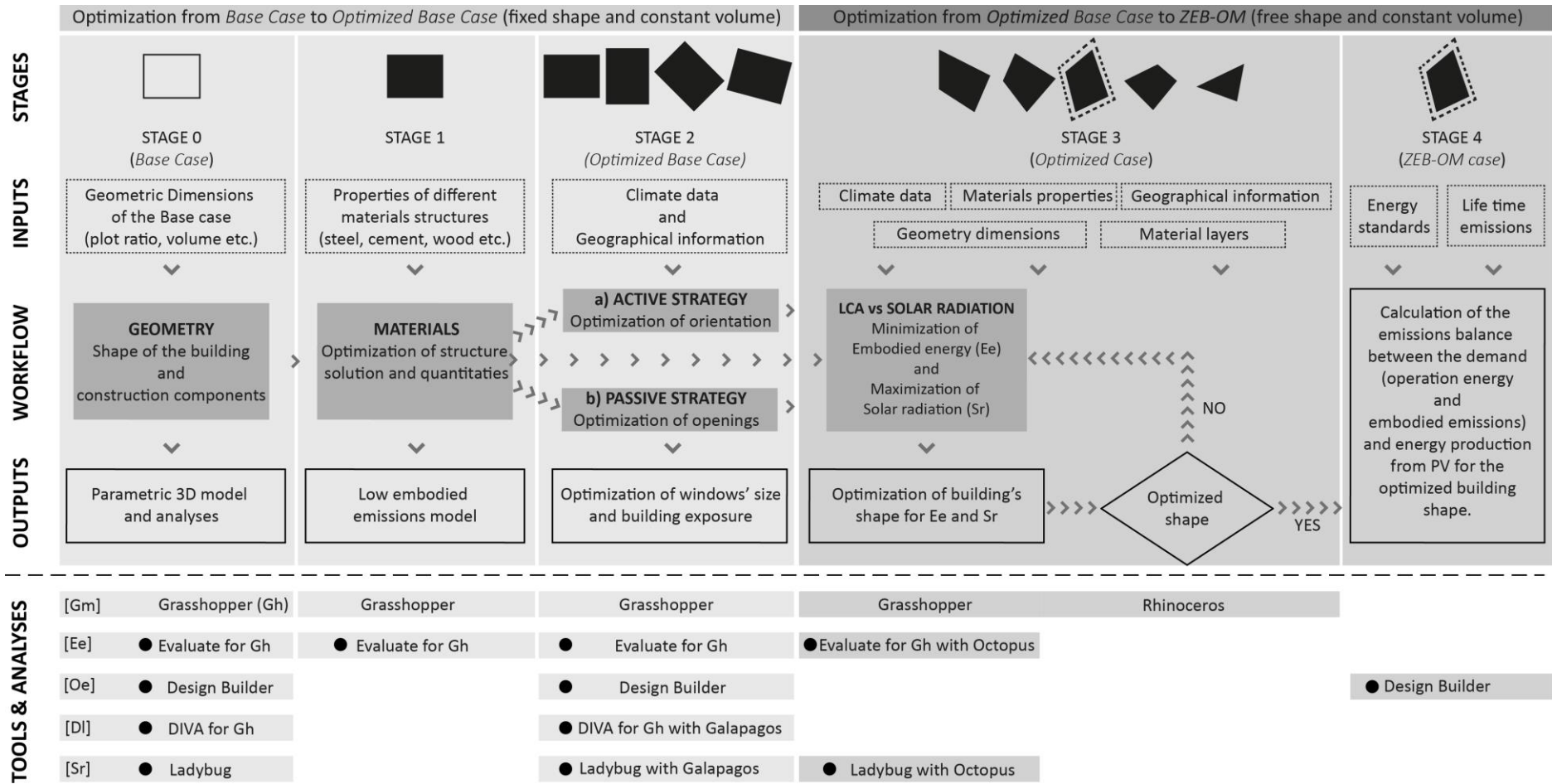
Figure 1. Flowchart of the methodology of the study: the top part shows the plan while the bottom part shows the tools used to control the geometry (Gm) and deal with the related environmental analyses such as embodied energy (Ee) and operational energy (Oe) as well as the energy analyses, such as solar radiation (Irr_{gl}) and daylight factor (Df), conducted in each stage.

1   3.1. *The ZEB case study building*

2   The process was applied to a single-family house concept building in Oslo (Norway) (Figure 2) which aims to

3   reach the ZEB–OM level [45, 47]. This concept building was used as the *Base Case* in this study.
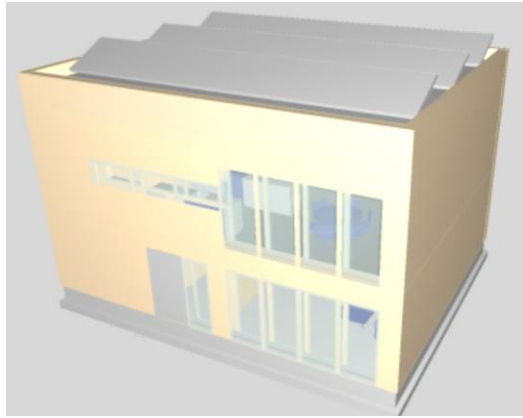
4

5   Figure 2. View of the ZEB concept building, called *Base Case* in this study.

6   The building is a two-story dwelling characterized by a box shape and a rectangular plan which is

7   approximately 10.0 m by 8.0 m, with the longest façades facing south and north. The building contains four

8   bedrooms and two bathrooms, which are arranged on two floors with a total heated floor area (HFA) (excluding

9   the external walls) of 160 m^2 (Figure 3).

10

11   Figure 3. Plans of the ground floor (left) and the first floor (right) of the *Base Case*.

12   The window openings account for an area of 36 m^2, which cover 35% of the façades, while the windows'

13   door-to-floor ratio is 22.5%. The characteristics of the construction of the *Base Case* are detailed in Table 3, and

14   the embodied emissions for its construction materials are listed in Table 4. The values of the energy

15   consumptions and GHG emissions for appliances are summarized in Table 5.

16   Table 3. Specification of the U-value of the different components of the ZEB concept building's envelope.

Components	U-values [W/m^2 K]	Thermal insulation detail
External wall	0.12	Timber wall with 350-mm-thick insulation
Roof	0.10	Compact roof with 400-mm-thick insulation
Slab on the ground	0.07 (0.06)	Floor construction with 500-mm-thick insulation, the value in brackets considers the thermal resistance of the ground
Windows	0.65	Triple-glazed low-energy windows, with insulated frame
Doors	0.65	Insulated doors

1

2 Table 4. Building elements of the ZEB concept included in the LCA calculation.

Building elements	GHG emissions [kg $CO_{2\text{-eq}}$ / m^2 HFA year]
Groundwork and foundations	1.44
Superstructure and outer walls	1.69
Inner walls	0.50
Structural deck	0.24
Outer roof	0.64
Heating distribution system and units	0.65
Ventilation system	0.05
Photovoltaic system	2.90
Solar thermal system	0.24
Total	**8.35**

3 Table 5. Load demand for various appliances included in the calculation [46].

Appliances	Energy consumption [kWh]	Operational emissions [kg $CO_{2\text{-eq}}$ / m^2 HFA year]
Dishwasher	234	0.19
Tumble dryer	320	0.26
Washing machine	189	0.15
Refrigerator	175	0.14
Freezer	234	0.19
Oven	160	0.13
TV (LED)	76	0.06
Other (lighting)	1000	0.81
Total	**2388**	**1.94**

4   The energy requirements are covered by an air-to-water heat pump that couples solar collectors on the façade

5 with a PV system installed on the flat roof. The selected PV system is oriented in a southerly direction at a tilted

6 angle of 40 degrees (Figure 2). Vacuum tube solar collectors are integrated on the vertical south façade. The total

7 solar thermal production has been estimated at more than 3,300 kWh/a for a PV system area of 8.3 m^2. The total

8 production of the PV system, which covers 69 m^2 of the roof, can reach more than 11,000 kWh/a. The air

9 handling unit is located in a storage room on the first floor with exhaust grills and air intake on the northern

10 façade.

11 Table 6. Specification of the HVAC systems [46].

12

13

14

15

System	Values	Solution
Heat recovery	η = 85.0 %	Rotary wheel heat exchanger
Specific fan power	SFP = 1.0 kW/(m^3/s)	Low-pressure AHU and low-pressure ducting system
Installed cooling capacity	Q''_{cool} = 0 W/m^2	No cooling
Installed heating capacity	Q''_{heat} = 18 W/m^2	Installed capacity for hydronic floor heating and radiators

16

17   The air handling unit is characterized by a rotary wheel exchanger with an efficiency of 85%, which allows

18 the conventional electric heating coil to be omitted. The heating system is hydronic and is characterized by two

19 different types of terminals: a heated floor in the bathroom and in the entrance, one for each floor. The

20 specification for the heating, ventilation and air conditioning (HVAC) systems are summarized in Table 6. The

21 water temperature in the hydronic system is set to 45°C and the seasonal performance factor is 2.25. The solar

22 thermal system is connected to a water tank, thus helping the heat pump to cover the thermal load. A

23 photovoltaic system is installed on the roof to balance the emissions given by the building's energy use for space

24 heating and appliances. The total energy demand for lighting during a year was set equal to 7.6 kWh/m^2, while

1   the specific annual energy demand for appliances was set to 14.9 kWh/m^2, with the energy demand for domestic

2   hot water of 30.0 kWh/m^2 per annum.

3   3.2. *Stage 0: Base Case building*

4   In the initial stage (stage 0), the *Base Case* and the entire load-bearing structure, building structural

5   components (i.e. pilots, slabs, external and internal walls, roof and basement), technological elements (i.e. doors,

6   windows and internal walls) and material layers were modeled with the graphical algorithm editor *Grasshopper*

7   [67] and are controlled parametrically. At the end of this stage, the analyses of embodied emissions, daylight

8   factor and global solar radiation were conducted on the *Base Case*. The outcomes were used as reference values

9   in the following stages of multi-objective optimization.

10   3.3. *Stage 1: correlation between structural solution and material quantities*

11   In stage 1, the process focused on the optimization of the structural solution and material quantities by

12   maintaining a constant volume for the *Base Case* house.

13   Three different construction systems were selected with main materials such as autoclaved aerated concrete

14   blocks (i.e. Ytong), clay bricks and timber frame (Table 7). The embodied emission factors for the materials

15   were extracted from the Norwegian Environmental Product Declarations (EPD) where available, otherwise from

16   the *Ecoinvent* LCA database. In this research, a dedicated generative algorithm, that constitutes one part of the

17   whole workflow, was developed to conduct an LCA parametrically through the *Evaluate component* tool in the

18   *Grasshopper* environment. The development of the LCA algorithm allowed several material properties to be

19   managed and enabled evaluation of the environmental impact of each material and technology on the resulting

20   embodied emissions and operational energy. In order to conduct LCA assessments, it was necessary to

21   individuate the functional unit and the calculation boundaries. The system boundaries used for the LCA

22   calculation in this study refer to those defined in the EN 15804; specifically, the stages A1–A5, B4, and B6 have

23   been used (Table 1). Phase B4 (replacement of building components) applies to the PV system only, which is

24   assumed to have a service life of 30 years. The functional unit—to which all the energy and environmental

25   impact calculation refer—is 1 m^2 of heater surface area (HFA). The building lifetime was set to 60 years, in

26   accordance with the Norwegian Standard 3940:2012 [68]. That part of the workflow that relates to LCA was

27   coupled to the first part of the workflow—the part which controls the variation of the building's geometry and

28   the building's components (walls, roof, slabs, windows etc.), which are constituted by different material layers

29   (see Table 7). The interface of the resulting workflow is divided into three main generative algorithms, capable

30   of parametrically controlling input data such as (i) building geometry (number of floors, length, width,

31   orientation, room height, window to wall ratio, etc.), (ii) properties of the material layers (e.g. thickness, volume,

32   density) and (iii) physical and environmental materials' features (functional unit, product service lifetime etc.).

33   The first step of the analysis was related to the calculation of the volume of the building components such as

34   walls, roof and slabs, which are constantly updated during the optimization process and are multiplied by the

35   density of the materials, before being converted into carbon emission by multiplying by the kgCO$_{2-eq}$/kg factor

36   from specific data (Norwegian EPDs) or generic data (*Ecoinvent*, *SimaPro* databases, etc.). A different

37   procedure was developed for those elements that cannot be measured by *Grasshopper*'s components. For

38   instance, the heating system was included in the calculation by considering the components (boiler, heat pump,

39   radiator, etc.) and their environmental impact. The embodied emissions, expressed in kgCO$_{2-eq}$/kg or m^3, were

1 calculated for the building lifetime of 60 years. The embodied emissions of the PV systems were multiplied by

2 two in order to account for their replacement every 30 years during the 60-year building lifetime.

3 Table 7. The building elements used in the analysis.

Roof					
Autoclaved aerated concrete blocks		**Clay**		**Timber**	
Layers	**Thickness (m)**	**Layers**	**Thickness (m)**	**Layers**	**Thickness (m)**
Outside		*Outside*		*Outside*	
		Asphalt	0.003	Asphalt	0.003
Asphalt	0.003	EPS insulation	0.350	EPS insulation	0.400
EPS insulation	0.400	Damp-proof membrane (LPDE)	0.001	Damp-proof membrane (LPDE)	0.001
Damp-proof membrane (LPDE)	0.001	Clay Later Energy	0.008	OSB board	0.015
Ytong deck	0.200	Timber frame (structural)	0.400 × 0.050	Timber frame (structural)	0.400 × 0.050
Gypsum plasterboard	0.013	Gypsum plasterboard	0.013	Gypsum plasterboard	0.013
Inside		*Inside*		*Inside*	
GHG emissions (kg $CO_{2\text{-eq}}$)	7.348	GHG emissions (kg $CO_{2\text{-eq}}$)	5.723	GHG emissions (kg $CO_{2\text{-eq}}$)	6.102

Outer walls					
Autoclaved aerated concrete blocks		**Clay**		**Timber**	
Layers	**Thickness (m)**	**Layers**	**Thickness (m)**	**Layers**	**Thickness (m)**
Outside		*Outside*		*Outside*	
		Pinewood cladding	0.020	Pinewood cladding	0.020
		Wind barrier	0.002	Wind barrier	0.001
		Glass wool insulation	0.200	Fibre cement board	0.015
Plaster	0.005	Damp-proof membrane (LPDE)	0.001	Glass wool insulation	0.350
Ytong energy + block	0.015	MDF board	0.003	Damp-proof membrane (LPDE)	0.001
Plaster	0.005	Timber frame (structural)	0.200 × 0.050	MDF board	0.003
Inside		Clay block	0.100	Timber frame (structural)	200 × 50
		Gypsum plasterboard	0.013	Gypsum plasterboard	0.013
		Inside		*Inside*	
GHG emissions (kg $CO_{2\text{-eq}}$)	6.918	GHG emissions (kg $CO_{2\text{-eq}}$)	8.575	GHG emissions (kg $CO_{2\text{-eq}}$)	8.792

Internal and ground floors					
Autoclaved aerated concrete blocks		**Clay**		**Timber**	
Layers	**Thickness (m)**	**Layers**	**Thickness (m)**	**Layers**	**Thickness (m)**
Inside		*Inside*		*Inside*	
		Wood flooring	0.013		
Wood flooring	0.013	MDF board	0.003	Wood flooring	0.013
MDF board	0.003	Timber frame (structural)	0.400 × 0.050	MDF board	0.003
Glass wool insulation	0.120	Glass wool insulation	0.120	Timber frame (structural)	0.400 × 0.050
Ytong deck	0.200	Clay tile (e.g. LaterEnergy)	0.060	Glass wool insulation	0.120
Gypsum plasterboard	0.013	Gypsum plasterboard	0.013	Gypsum plasterboard	0.013
Wood cladding	0.020	Pinewood cladding		Pinewood cladding	0.020
Outside		*Outside*		*Outside*	
GHG emissions (kg $CO_{2\text{-eq}}$)	4.116	GHG emissions (kg $CO_{2\text{-eq}}$)	2.181	GHG emissions (kg $CO_{2\text{-eq}}$)	2.314

1   Table 8. Main settings chosen for calculating operational energy in the *Design Builder* environment.

Design Builder settings	
Location	Oslo, Norway
Latitude	59° 54' 45 N
Longitude	10° 44' 45 E
AMSL height (m)	23
Summer set-point temperature (°C)	24
Winter set-point temperature (°C)	22
Natural ventilation (ACH)	2.5
Air infiltration (ACH)	0.5
Lighting (lux)	200
Heating system's terminals	Underfloor heating
Supplied energy	Air-to-water HP + solar thermal collectors + PV system
Occupational regime	Residence (single-family house)

2   Finally, the building energy consumption and the emissions related to the operational stage were estimated by

3   employing the *EnergyPlus* engine through the graphical user interface (GUI) of *Design Builder*. The geometry of

4   the *Base Case* model was imported from the Windows®-based NURBS *Rhinoceros* [69]. The settings requested

5   by *Design Builder* can be grouped into a number of categories: geographic (i), geometric (ii), physical (iii), and

6   user-related (iv) (Table 8). The location was set by defining the *EnergyPlus* weather file (.epw) for Oslo and

7   evaluating the boundary conditions of the model in terms of temperature and solar loading [70]. The ZEB

8   emission factor for the electricity grid mix used in the *Base Case* model was 0.132 kg $CO_{2\text{-eq}}$/kWh [71]. The

9   geometric model was coupled with information concerning the materials (Table 3) and the building elements

10   (Table 7). The analyses enable the thermal capacity of the building envelope to be assessed, as well as the heat

11   gains and losses through it. Furthermore, the total emissions balance and impact on embodied emissions of

12   materials, as well as emissions from operational energy use were determined for the building's lifetime. The

13   operational emissions (which contribute to the emission balance) have been taken into account in the calculation

14   as well as all the energy systems (heat pump system, fans and pumps, lighting, appliances etc.) installed in the

15   *Base Case*. Similarly, the avoided emissions due to PV system energy production in situ were measured by

16   applying the same weighting ZEB emission factor (symmetrical approach). All the values were included in the

17   emissions balance in order to determine the ZEB emissions level at the different stages.

18   3.4. *Stage 2: active and passive strategies*

19   The workflow of this stage was focused on the multi-objective optimization process applied to the building's

20   shape in order to enhance (i) passive and (ii) active strategies for the ZEB concept building.

21   For the active strategy, the orientation of the *Base Case* model was optimized in order to increase the global

22   solar radiation incident on the building envelope and to improve the energy production from the PV system. The

23   optimal building orientation was achieved by using the *Ladybug* [72] open-source plugin for *Grasshopper,*

24   which uses a standard (.epw) file. A set of iterative solar radiation simulations were conducted by varying the

25   orientation of the buildings—ranging from 0° (North) to 180° (South). This set of simulations were performed

26   using *Galapagos*, an evolutionary solver for *Grasshopper*, which allows the optimization of one objective

27   function, defined as 'fitness', each time, by automatically varying the values of the selected parameter, defined

28   as 'genome', which represents the parameters' variations (genes). In this case, the orientation of the building was

29   varied, as a selected genome, in order to obtain the maximum global solar radiation (fitness) on two contiguous

30   façades of the *Base Case* concept building. The same methodology was used for the passive strategy by setting

the adequate level of daylight factor (Df ≥ 2.5%) as 'fitness' in *Galapagos* to obtain the minimum amount of glazed surface. To achieve this, the size and the position of the windows were defined as genes. In order to control and manage these parameters, the building envelope was divided into heterogeneous cells by using the *Substrate* component [73] for *Grasshopper*.

Table 9. Set of 'rtrace' parameters used in the Radiance-based simulations for Df analysis.

Ambient bounces	Ambient divisions	Ambient super samples	Ambient resolution	Ambient accuracy
5	1024	16	256	0.10

Table 10. Material properties used in the Radiance-based simulations for ceiling, floor, walls and glazing surfaces.

Description	Material/colors	Radiance material	RGB*	Specularity**	Roughness***
Ceiling	Opaque/ clear brown	Wood generic ceiling (lightwood)	0.5/0.3/0.2	0.02	0.05
Floor		Wood generic floor (lightwood)			
Wall		Wood generic interior wall (lightwood)			
Single glazing	Translucent	Glazing single panel	0.96/0.96/0.96		

*RGB: the three components of the colors red (R), green (G) and blue (B). For each of the components, the value varies from 0.0 (no presence of color) to 1.0 (fully colored). For translucent material such as glass, the RGB code defines the transmission of the glazed surface and the value varies from 0.0 (a completely black surface) to 1.0 (a transparent surface).
**Specularity: the fraction of incident light that is reflected; varying from 0.0 for a perfectly diffusive surface to 1.0 for a perfect mirror.
*** Roughness: surface irregularities, that are quantified by the deviation in the direction of the normal vector of a real surface from its ideal form; it varies from 0.0 (perfectly smooth surface) to 1.0 (perfectly irregular surface).

The *Substrate component* works by generating cells based on a few randomly selected starting points. The areas near these points end up with the highest density of lines. The resulting grid determines the final position and the size of the glazed surfaces on the different façades of the building envelope. The process was managed by coupling *Galapagos* with a plugin for daylighting assessment, named *DIVA-for-Grasshopper*. It is an extension of *DIVA-for-Rhino*; a validated *Radiance*-based software that models the annual amount of daylight in and around buildings [74]. *DIVA-for-Rhino* is used as the calculation engine to obtain climate-based daylighting metrics [75], it is a *Daysim* calculation method, that uses typical weather data for a specific site location. The level of daylight was calculated on the horizontal work plane, placed at height of 0.90 m above the floor level. The set of *Radiance* simulation parameters (Table 9) was chosen by referring to similar studies in literature [76, 77], while *Radiance* primitives were set to simulate typical Norwegian indoor materials (Table 10). At the end of this stage, energy (i.e. solar radiation and daylight factor analysis) and environmental (i.e. embodied emission and operational energy) analyses were conducted on the *Optimized Base Case* and compared with the *Base Case*. All the geometry transformations and analyses prior to this stage were made by maintaining both the shape and the volume of the *Base Case* at constant levels.

3.5. *Stage 3: balancing solar global radiation and LCA*

In stage 3, the workflow was developed in order to enable modification of the shape of the *Base Case* by maintaining the volume of the building constant. The shape's variation represents the core of this part of the workflow, in which parametric design was used to reach the level of ZEB–OM by balancing the maximization of solar radiation on the building envelope with the minimization of the embodied and operational emissions. Both aspects were set as objective functions (fitness) of the evolutionary solver *Octopus*. Similar to *Galapagos*, *Octopus* works with genome and fitness but it also allows optimization of several objective functions simultaneously within a single multi-objective optimization process. It starts working by creating an initial

1 population of optimized building shapes through multiple-crossovers mutations and with random combinations

2 of genes. The best solutions that meet the fitness criteria are then selected. The optimization process runs until

3 the final population of optimized building shapes solutions has been generated.

4 Table 11. Set of 'rtrace' parameters used in the Radiance-based simulations for grid-based radiation maps analysis.

Ambient bounces	Ambient divisions	Ambient super samples	Ambient resolution	Ambient accuracy	Specular threshold Direct sampling	Specular threshold Direct sampling	Direct relays
3	1000	20	300	0.10	0.15	0.20	2

5 In this study, *Octopus* was employed to control specified coordinates, corresponding to the definition of the

6 geometry of the building; these were managed in order to generate the most responsive configurations in terms

7 of both global incident solar radiation and embodied emissions (fitness). The shape of the *Base Case* concept

8 building was modeled following a parametric approach, which enabled several building shapes to be obtained by

9 varying input parameters (i.e. control-point coordinates) to optimize solar radiation and to minimize material

10 quantities and embodied emissions. Finally, the calculation of annual global solar radiation incident at the

11 building envelope was estimated using the *Ladybug* software tool. Iterative grid-based radiation map analyses

12 were performed by setting 'rtrace' parameters in *Radiance* (Table 11) to values found in similar previous studies

13 [78, 79]. Regarding the LCA of the *Optimized Base Case*, the same workflow described in stage 1 was also used

14 in this stage, while the operational energy was estimated in *Design Builder*.

15 4. **Results and discussion**

16 The results are organized in the same aforementioned sequence of stages, in order to better estimate the

17 impact of each stage in terms of energy emission balance between energy production through active systems

18 (such as photovoltaic (PV) panels) and operational emissions.

19 4.1. *Stage 0: ZEB Base Case*

20 The emissions embodied in materials for the *Base Case* were calculated to be equal to 8.35 kg $CO_{2\text{-}eq}$/m^2 HFA

21 per year (80,205 kg $CO_{2\text{-}eq}$, total emissions for 60 years), while the emissions related to the operational stage

22 were found to be equal to 5.0 kg $CO_{2\text{-}eq}$/m^2 HFA per year. Finally, the PV system placed on the flat roof resulted

23 in avoided emissions equivalent to 9.3 kg $CO_{2\text{-}eq}$/m^2 HFA per year.

24 4.2. *Stage 1: calculation of the embodied energy for the Base Case*

25 At stage 1, the calculation of the embodied emissions was performed in the *Base Case* concept model for the

26 analyzed materials (autoclaved aerated concrete blocks (Ytong), clay bricks and timber) in order to define their

27 environmental impact (Figure 4a). The use of autoclaved aerated concrete blocks (i.e. Ytong), gave 83,850 kg

28 $CO_{2\text{-}eq}$ (8.75 kg $CO_{2\text{-}eq}$/m^2 HFA per year), which is higher than the embodied emissions of the *Base Case* (80,200

29 kg $CO_{2\text{-}eq}$, equal to 8.35 kg $CO_{2\text{-}eq}$/m^2 HFA per year) (Figure 4a). Nevertheless, these blocks enabled the lowest

30 value of embodied emissions on the outer walls (6,915 kg $CO_{2\text{-}eq}$) given their low thermal conductivity (0.21

31 W/m K) which obviates the need for a thermal insulation layer that is required in the other solutions. This means

32 that for the outer walls only, the autoclaved aerated concrete block solution led to 57% reduction in emissions

33 compared to those given by the *Base Case* (Figure 4b).
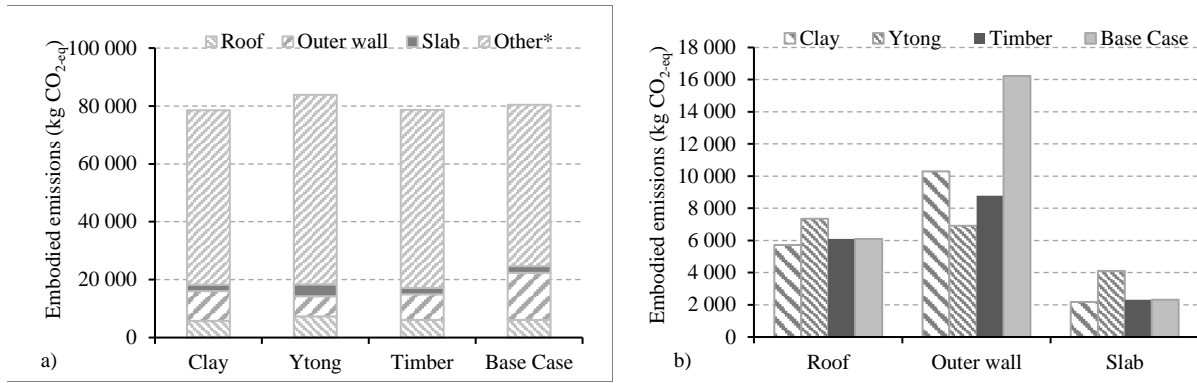
1   * This includes all of the elements that are not specified on the other three classes, such as photovoltaic panels, foundation and systems.

2   Figure 4. (a) The total emissions according to bearing structure. The embodied emissions were estimated for a lifetime of 60 years.
3   Embodied emissions of the model with a 0.60 m by 0.60 m module are split in order to consider the impact of each material on a single
4   technological component (b).

5   The lowest embodied emissions were achieved with clay bricks, resulting in emissions of 78,500 kg CO_{2-eq}
6   (8.18 kg CO_{2-eq}/m^2 HFA per year). These values are close to those given by the timber frame construction
7   (78,700 kg CO_{2-eq} equal to 8.20 kg CO_{2-eq}/m^2 HFA per year). Considering the incidence of embodied emissions
8   given by the outer walls, it was found that for a timber system, the GHG embodied emissions are 18% less
9   (8,700 kg CO_{2-eq}) than those given by using clay bricks (10,300 kg CO_{2-eq}). Furthermore, the fact that timber is a
10 more locally available material in Norway represents a significant advantage in relation to the emissions from
11 production (due to the low-carbon grid), and from transportation (due to the close proximity to the site of the raw
12 materials' production). Based on these findings, the timber frame model was selected to be further analyzed in
13 the next stages of the multi-objective optimization process of this study.

14   4.3. *Stage 2: Optimized Base Case*
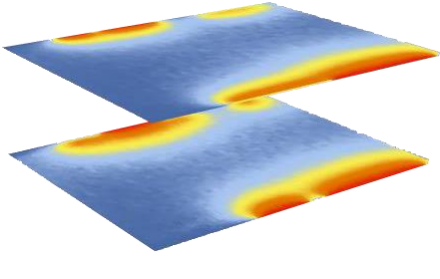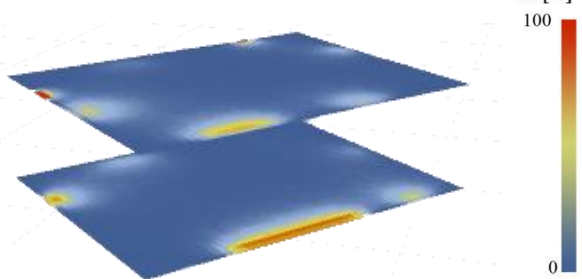
15   In stage 2, the process was focused on the optimization of active and passive strategies in the *Base Case*.

16

17 Figure 5. Stage 2 – *Optimized Base Case*: the ground floor (left) and the first floor (right) with the optimized orientation and the new inner
18 distribution of the spaces.

The results of the analyses indicated that the best-optimized orientation corresponds to the orientation northwest–southeast, which is given by a rotation of the plan about 51° from the horizontal direction (0°), as shown in Figure 5.

Table 12. Comparison of the daylight factor maps for the *Base Case* and the *Optimized Base Case,* generated by the *DIVA-for-Grasshopper*.

	Base Case	Optimized Base Case
		Df [%] 100 0
Df* (%)	7.5	2.5**
Ratio window to wall	34.7	5.6
Glazed surface (m²)	40.5	11.5

* Average value considering the HFA surface.

** Chosen in accordance with specific regulation and best practices in Norway.

The optimized orientation allows for 194,000 kWh/a of total global solar radiation on the building envelope: 77,000 kWh/a is incident on two contiguous façades oriented southwest and southeast, while the other two façades, oriented northwest and northeast, collect 33,000 kWh/a. A total of 84,000 kWh/a of solar global radiation is incident on the flat roof. These outcomes are aligned with previous studies conducted at high latitude [80, 81, 82, 83]. The total value of the global incident solar radiation on the two contiguous and most-radiated façades, oriented southwest and southeast, is 10% higher compared to that of the *Base Case* north–south orientation, which generated about 69,000 kWh/a. Some of the benefits of the optimized orientation manifest in (i) the exploitation of the global solar radiation on the contiguous southwest and southeast façades for additional installation of PV panels and (ii) the reorganization of the layout of the two floors. In this stage, the inner distributions of the functions of the *Base Case* have been rearranged: the distribution and service spaces (i.e. hall, utility room, stairwell, corridor, bathroom) were moved to the northern zones, while the served spaces (i.e. dining room, living room, bedroom) were located in the southern areas, characterized by a better sun exposure (Figure 7). Consequently, regarding the optimization of the passive strategy, the minimization of the size of the windows and their position on the façades was optimized in order to: (i) guarantee an adequate level of daylighting and (ii) reduce the heat losses from the openings, which affect the emissions balance of the entire building. The comparison between the *Base Case* and the *Optimized Base Case* highlighted that the area of glazing could be reduced about 70% (from 40.5 m² in the *Base Case* to 11.5 m² in the *Optimized Base Case*) while still guaranteeing the required minimum value for daylight factor (Df $\geq$ 2.5 %) [84] (Table 12). These results align with Norwegian best practice regulations for residential buildings. Furthermore, the lower quantity of glazing in the *Optimized Base Case* allows for a consistent reduction of the building's energy losses. However, this point highlights the importance of the role of the designer in considering the parametric solutions in a complete and holistic design approach. In terms of carbon footprint, it led toward the reduction of both embodied and operational emissions. In particular, embodied emissions (Ee) were reduced from 78,000 kg $CO_{2\text{-}eq}$ (8.20 kg $CO_{2\text{-}eq}$/m² HFA per year)—corresponding to the timber enhanced model—to 74,000 kg $CO_{2\text{-}eq}$ (7.68

1   kg $CO_{2\text{-eq}}$/m^2 HFA per year). The emissions from operational energy (Oe) were decreased from 5.00 kg $CO_{2\text{-eq}}$/m^2 HFA per year to 4.60 kg $CO_{2\text{-eq}}$/m^2 HFA per year.

2

3   Table 13. Variation of the emission balance depending on the percentage of covered PV systems on the two most radiated and contiguous

4   façades (southwest and southeast) of the *Optimized Base Case*.

Percentage of the available surface covered by PV panels (%)	0	10	20	30	40	50	60	70	80	90	100
PV panels added (m^2)	0	10.5	21.0	31.5	42.0	52.5	63.0	73.5	84.0	94.5	105.0
PV system production* (kg $CO_{2\text{-eq}}$/m^2 HFA per year)	9.2	10.4	11.7	12.9	14.2	15.4	16.7	17.9	19.2	20.4	21.7
Ee* (kg $CO_{2\text{-eq}}$/m^2 HFA per year)	7.7	8.1	8.6	9.0	9.4	9.9	10.3	10.7	11.2	11.6	12.0
Oe* (kg $CO_{2\text{-eq}}$/m^2 HFA per year)	4.6	4.6	4.6	4.6	4.6	4.6	4.6	4.6	4.6	4.6	4.6
Balance (kg $CO_{2\text{-eq}}$/m^2 HFA per year)	-3.1	-2.3	-1.5	-0.6	0.2	1.0	1.8	2.6	3.4	4.2	5.0

5   * The unit considered is kg $CO_{2\text{-eq}}$/m^2 HFA per year, which is evaluated based on a building lifetime of 60 years and an HFA of 160 m^2.

6   The *Base Case* already has 69 m^2 of PV panels installed on the roof and vacuum tube solar collectors installed

7   on the façades; however, the ZEB–OM level is only achieved with the additional surface available for PV

8   systems. In this regard, a calculation of total surface of installed PV system required on the façades of the

9   *Optimized Base Case* in order to achieve the ZEB–OM level has been conducted (Figure 6a). The total net

10 available area for installing the PV systems considered the contiguous façades southwest and southeast suitable

11 accounts 105m^2. Table 13 summarizes the variation of the emission balance according to the percentage of

12 covered PV panels on these façades.
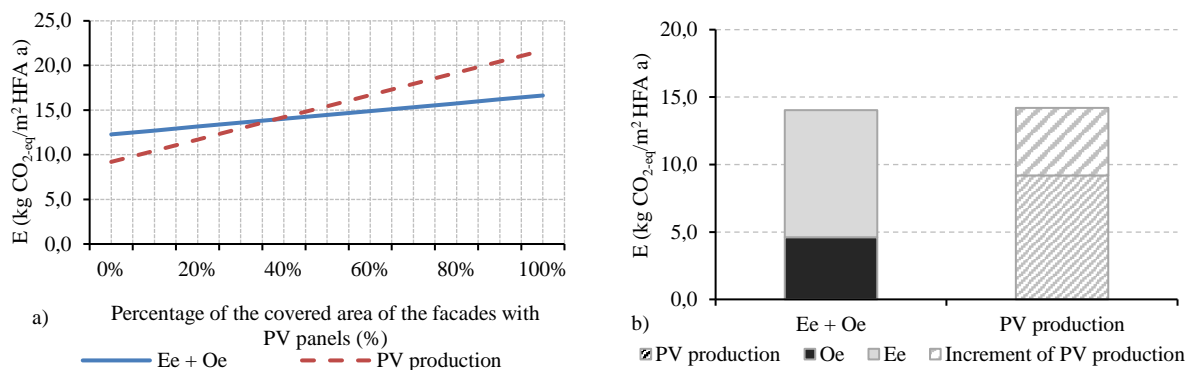
13 Figure 6. (a) Variation of the emission balance with the percentage of available areas of the façade covered by PV panels. (b). Operational

14 emissions balance considering only the PV system installed on the roof of the *Base Case* without adding BIPV system installed on the

15 façades and considering the BIPV system on the façade.

16   In this calculation, the variation of the embodied emissions (Ee) due to the PV panels has been included. In

17 Figure 6a, the continuous line describes the variation of embodied and operational emissions (Ee + Oe) that equal

18 0.04 kg $CO_{2\text{-eq}}$/m^2 HFA per year, while the dashed line indicates the energy production for each square meter of

19 PV system corresponding to 0.12 kg $CO_{2\text{-eq}}$/m^2 HFA per year. It should be noted that the embodied emissions

20 from the materials used in the PV system installation, as well as the energy production from this system, have

21 been counted as a base load due to the PV panels, which are already installed on the roof in the *Base Case*. The

22 analysis found that covering all 105 m^2 of the contiguous façades facing southwest and southeast with PV panels

23 results in a positive mismatch of 5.00 kg $CO_{2\text{-eq}}$/m^2 HFA per year in terms of the emissions balance, while the

24 ZEB–OM level is reached by covering approximately 45% of the available surface with PV panels. Therefore, in

1 the *Optimized Base Case*, by adding 45 m^2 of PV panels on the two most-radiated and contiguous façades

2 (Figure 7), it is possible to counterbalance the sum of embodied emissions for the building materials and

3 emissions from operational energy with the on-site energy production (Figure 6b).
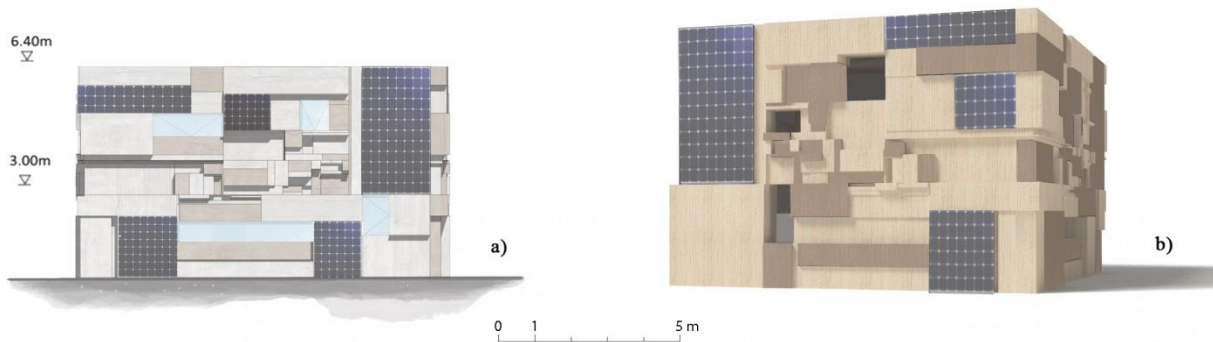
4

5 Figure 7. Stage 2 – *Optimized Base Case*: the elevation of the southwest façade (a) and the 3D view of the model of the southeast façade with

6 PV panels integrated on the façade (b).

7 ### 4.4. *Stage 3: Optimized Case*

8 The outcomes from the previous stage regarding the best orientation were used as a fixed input in stage 3,

9 which is focused on the optimization of the building's shape. A series of iterative analyses were performed,

10 using the *Octopus* evolutionary solver, in order to achieve the optimal shape for the multi-objective functions,

11 relative to the defined parameters. This shape would be the most environmentally responsive with the lowest

12 impact on embodied emissions from materials and operational emissions, as well as being the most energetically

13 productive. The *Octopus* software generated and compared a multitude of different model shapes, which were

14 grouped into generations of solutions. All the optimized outcomes, according to the multi-objective optimization,

15 have been graphically represented in Figure 8, in which the ten best-optimized shapes have been highlighted. In

16 Figure 9, these latter outcomes have been converted into a common unit area and annualized to enable estimation
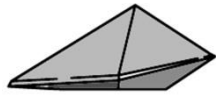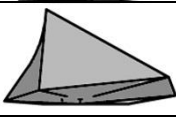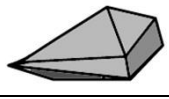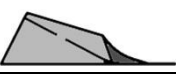
17 of emissions.
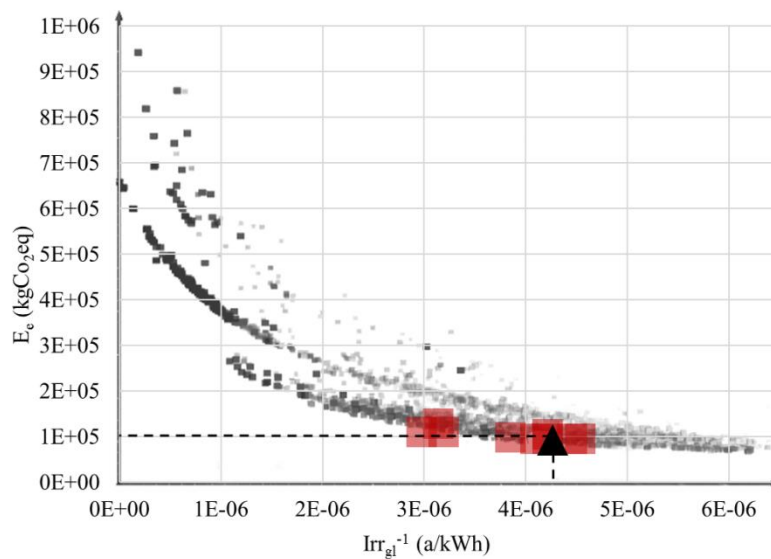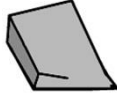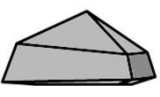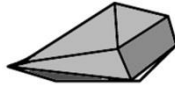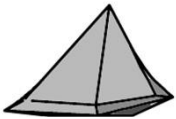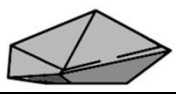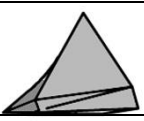
18

19 Figure 8. Graphical representation of the outcomes of the multi-objective optimization; the ten most-optimized shapes are shown by the

20 square markers, while the most-optimal shape is pinpointed by the triangular marker and dashed lines.
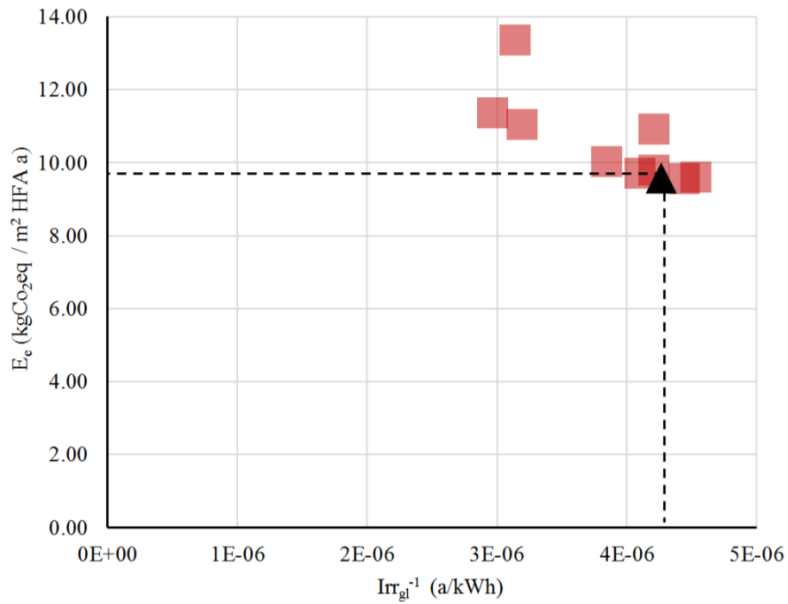
1
2 Figure 9. Graphical representation of the ten most-optimized shapes, converted into the common unit area and annualized to enable
3 emissions estimation. As in Figure 8, the ten most-optimized shapes are shown by the square markers, while the most-optimal shape is
4 pinpointed by the triangular marker and dashed lines.

5   The selected best shapes results are clearly influenced by the sun's path in Oslo, which changes significantly

6 during the year. In fact, the sun height at noon in Oslo varies from around 55° in the summer to below 10° in the

7 winter. Indeed, the main surfaces were characterized by tilt angles up to 60° from the horizontal, which allows

8 the low sun-angle rays, typical at these latitudes, to be caught by the surfaces of the building's envelope.

9 Table 14. Elevation of the optimized models carried out from the multi-objective optimization process developed with the *Octopus*
10 evolutionary solver.

| Octopus output	Irr_{gl} (kWh/a)	Ee (kg CO_2eq)	Shape	Octopus output	Irr_{gl} (kWh/a)	Ee (kg CO_2eq)	Shape
Output 1	243,300	93,000		Output 6	220,400	92,000	
Output 2	234.500	92,000		Output 7	237,200	104,350	
Output 3	237,100	93,800		Output 8	312,600	106,000	
Output 4	259,650	96,200		Output 9	336,600	108,950	
Output 5	224,500	91,450		Output 10	317,450	128,000	

11   Therefore, the quantity of global incident solar radiation on the building envelope caught by the best-

12 optimized shapes could vary from around 220,000 kWh/a (output 6 in Table 14) to 336,000 kWh/a (output 9 in

13 Table 14). The best-optimized shapes (listed in Table 14) provide significant improvements in terms of solar

20

global radiation, which varies from 14% (output 6) to 74% (output 9) compared to the *Base Case* (193,000 kWh/a). Among the best-optimized shapes, output 2 was chosen as the best *Optimized Case* by considering the energy and environmental optimization as well as the design solution and the user implications in terms of usable space. Of all the various outputs, this shape most successfully meets both the multi-objective optimization (i.e. maximization of Irr_{gl} and reduction of Ee) while also being suitable in terms of interior spatial distribution. The shape of output 2 enables 234,500 kWh/a to be caught, which means an improvement of more than 20% in comparison to the *Base Case.*

Table 15. Comparison of global incident solar radiation (Irr_{gl}) and daylight factor (Df) for *Base Case* (Stage 0), *Optimized Case* (Stage 3) and *ZEB–OM Case* (Stage 4).

Components	Stage 0	Stage 3	Stage 4
	Base Case	*Optimized Case*	*ZEB–OM Case*
Irr_{gl} roof (kWh/a)	83,000	122,500	99,000
Irr_{gl} façades (kWh/a)	110,000	112,000	174,000
Irr_{gl} roof and façades (kWh/a)	193,000	234,500	273,500
Df (%)	7.5	10	
Ratio window to wall	34.7	10	
Glazed surface (m^2)	40.5	39	

However, some adjustments were considered necessary in order to maintain the original spaces in the constant heated volume (equal to the *Base Case*). By taking these adjustments into account, the final optimized shape receives 273,500 kWh/a, thus enabling an improvement of more than 40% on the *Base Case*, as shown in Table 15.
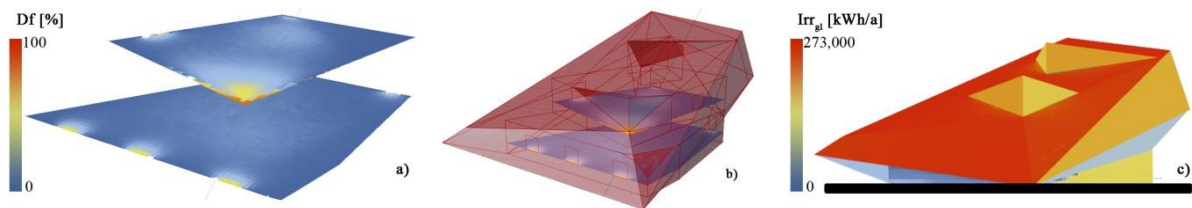
Figure 10. Visualization of the (a) Df analyses, (b) Grasshopper geometry and (c) global incident solar radiation on the *ZEB–OM Case.*

Regarding the variation in the Df in the two levels of the *Optimized Case* (Figure 10), it was found that, in comparison to the *Base Case*, the optimized exposure and distribution of the openings contributes to increasing the daylight factor. This resulted in an increase equal to 10% in the *Optimized Case*, compared to 7.5% in the *Base Case*, even if the window area was approximately the same: 39 m^2 in the *Optimized Case* and 40.5 m^2 for the *Base Case*.

4.5. *Stage 4: Embodied emissions and operational energy of the Optimized Case*

The level of embodied emissions for the *Optimized Case* was calculated as 87,400 kg CO_{2-eq} (9.11 kg CO_{2-eq}/m^2 HFA per year)—8% higher than the initial *Base Case* concept project (80,400 kg CO_{2-eq} equal to 8.35 kg CO_{2-eq}/m^2 HFA per year). This variation is mostly due to the increase in total surface area of the building envelope, from 386 m^2 to 460 m^2.

It is worth underlining that this variation was an expected outcome, given that the heated volume of the building was kept constant. One of the declared strategies to reach the level of the ZEB–OM was to maximize the solar global radiation through the optimization of the building's shape. In this regard, the multi-objective optimization process contributed to the creation of a new shape, characterized by improved exposure of the

entire building envelope, while also enabling an almost doubling of the available area for installing solar active systems, from 69 m² in the *Base Case*, to 173 m² in the *Optimized Case* (Table 16).

Table 16. Variation of the emission balance according to the percentage of covered PV systems on the two most-radiated and contiguous façades of the *Optimized Case*.

Available surface*		173 m²										
PV panels added	(%)	0	10	20	30	40	50	60	70	80	90	100
	(m²)	0.0	17.3	34.6	51.9	69.2	86.5	103.8	121.1	138.4	155.7	173.0
PV system production** (kg CO$_{2\text{-eq}}$/m² HFA per year)		0.0	2.9	5.8	8.7	11.6	14.5	17.4	20.2	23.1	26.0	28.9
Ee** (kg CO$_{2\text{-eq}}$/m² HFA per year)		6.2	7.0	7.7	8.4	9.1	9.8	10.5	11.3	12.0	12.7	13.4
Oe** (kg CO$_{2\text{-eq}}$/m² HFA per year)		9.7	9.7	9.7	9.7	9.7	9.7	9.7	9.7	9.7	9.7	9.7
Balance (kg CO$_{2\text{-eq}}$/m² HFA per year)		-15.9	-13.8	-11.6	-9.4	-7.2	-5.1	-2.9	-0.7	1.5	3.6	5.8

* Considered on the two contiguous façades, southwest and southeast.

** The unit considered is kg CO_2eq/m²HFA per year, which is evaluated based on the building's lifetime of 60 years and an HFA of 160 m².
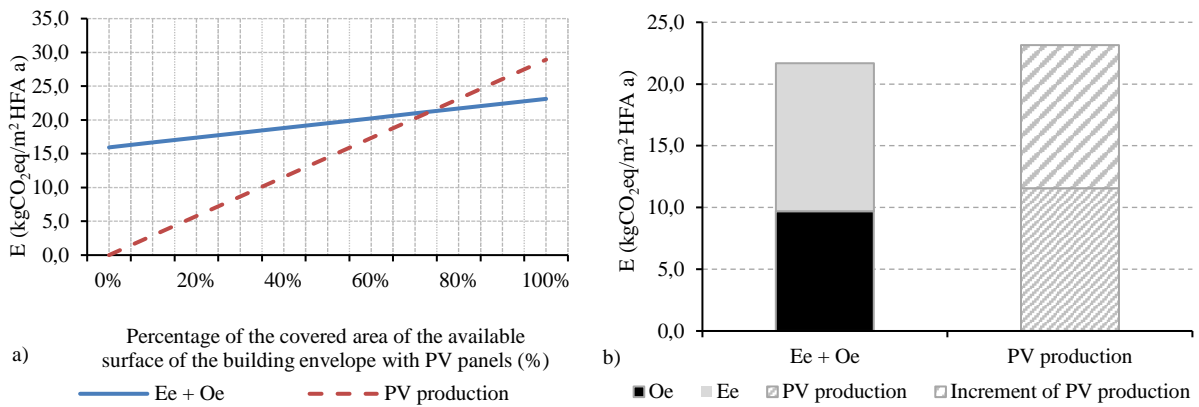
Figure 11(a). Variation of emissions balance according to the percentage of available areas of the building envelope covered by PV panels.

(b). Operational emissions balance considering the PV system installed on the building envelope of the *Optimized Case* for a surface equivalent of the PV system installed on the roof of the *Base Case* (69 m²) and by covering 75% (equal to 130 m²) of the available surface with BIPV.

Even if the PV production is 20% higher than the *Base Case*, the total emission (Ee + Oe) is more than double that of the *Base Case* (Figure 11b). Therefore, in order to reach the level of ZEB–OM in the *Optimized Case*, a total surface equal to 75% of the available area (equivalent to 130 m²), should be covered by PV panels (Figure 11a). In terms of emission balance, this latter solution presents higher total emissions (Ee + Oe), equal to 21.7 kg CO$_{2\text{-eq}}$/m² HFA per year, compared to the *Base Case*, but the energy production from PV system is equal to 23.1 kg CO$_{2\text{-eq}}$/m² HFA per year. Therefore, this solution covers the total emissions as well as enabling the level of ZEB–OM to be reached (Figure 11b). The southwest (a) and southeast (b) elevations, and the section (c) of the final design proposal of the *Optimized Case* have been visualized in Figure 12, while the 3D visualization of the final design are shown in Figure 13. The building envelope is to be covered by the amount of PV panels that enables the achievement of the ZEB–OM level, while timber elements are used for the structure and the cladding.
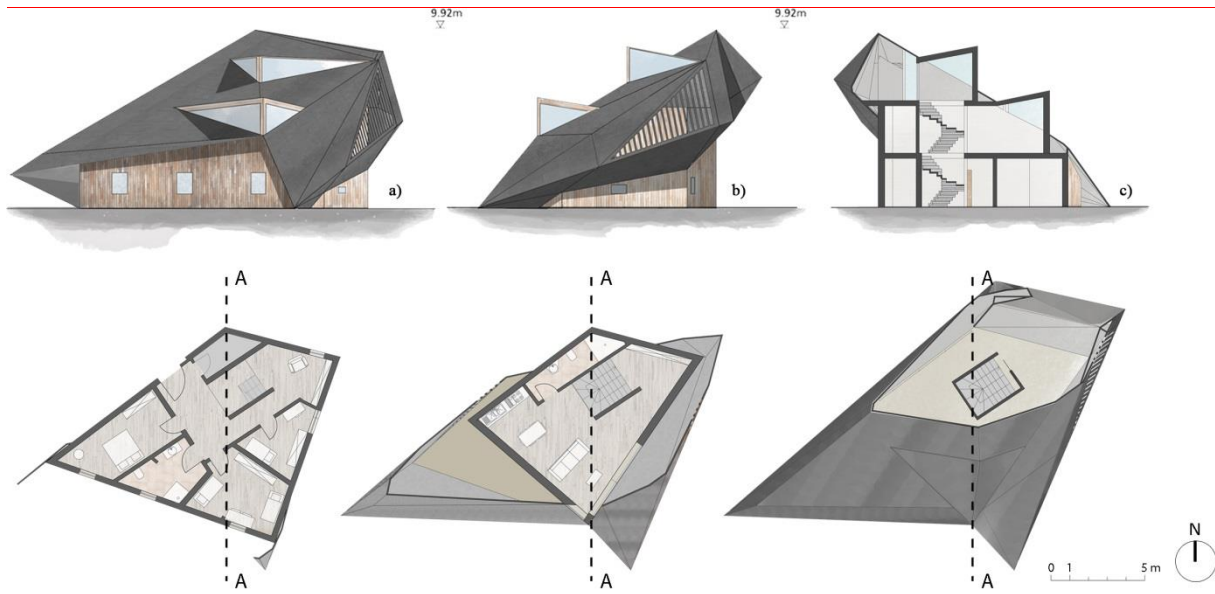
Figure 12. On top, the southwest (a) and southeast (b) elevation and section (c). On the bottom, the ground floor (left), first floor (center) and the roof floor (right) for the *Optimized Case* (end of stage 4).

Figure 13. View of the 3D model of the building at the end of the stage 4: southwest view (a) south view (b) and southeast view (c).

### 4.6. *Evolution of the shape and comparison between the stages*

The optimization process described in this paper has demonstrated the suitability of a parametric design for minimizing the GHG emissions of a ZEB. Stage by stage, the building's components were investigated and optimized, with particular focus on embodied emissions, operational emissions, daylighting and global irradiation. The results, presented and discussed in detail in the preceding paragraphs, are summarized in Table 17.

Table 17. Overview of the results achieved through the optimization process described in this paper.

		Stage 0	Stage 1	Stage 2	Stage 3	Stage 4
		(Base Case)	*(Base Case)*	*(Optimized Base Case)*	*(Optimized Case)*	*(ZEB–OM Case)*
Ee	(kgCO$_2$. eq/m^2 HFA per year)	8.35	8.20	9.40	9.58	12.00
Oe		5.00	5.00	4.60	9.70	9.70
PV (panel surface area)		9.30 (69 m^2)	9.30 (69 m^2)	14.20 (111 m^2)	20.2 (121 m^2)	23.10 (138 m^2)
Emissions balance		- 4.05	-3.90	0.20	0.92	1.40
Irr$_{gl}$	(kWh/a)	193,000	193,000	194,000	234,500	273,500
Df	(%)	7.5	7.5	2.5	10.0	10.0
Glazed surface	(m^2)	40.5	40.5	11.5	39.0	39.0

Although the Ee mainly increases stage by stage, along with Oe, the optimized model is already able to achieve the ZEB–OM ambition level at stage 2, due to the increase in both the PV plant's extension and the Irr$_{gl}$

23

1 received. In fact, both Ee and Oe increase with the optimization of the building shape, changing from a compact
2 one (stage 0, *Base Case*) to the final design (stage 4, *ZEB–OM Case*), characterized by a more extensive
3 envelope. However, the improved exposure achieved in the final stage by employing evolutionary solvers
4 enabled a reduction in the glazed surface, while maintaining an adequate visual comfort level derived from stage
5 2 (*Optimized Base Case*) along with an increasing of the Df with a constant glazed surface, carried out from
6 stage 3 (*Optimized Case*). In Figure 14, a comparison between the total emissions in the different stages is
7 presented: it is clearly shown that from stage 2, the optimization process increases the total emission given by Ee
8 and Oe (Figure 14a). However, it has to be noted that from stage 2, the emissions released in atmosphere (Ee and
9 Oe) are counterbalanced by the energy production provided by the PV system (i.e. in the total emission balance
10 the energy production from PV system has been considered as avoided emissions by using the electricity-to-
11 emissions conversion factor) (Figure 14b)—it is this which enables the level of ZEB–OM to be reached.

a)

b)
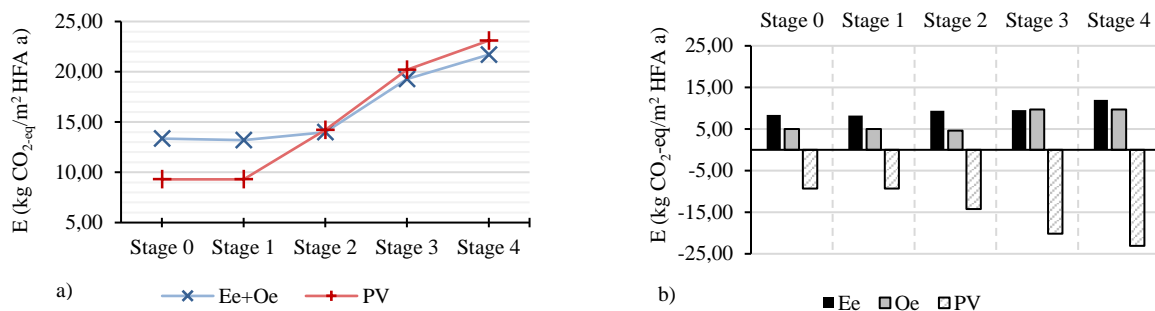
12 Figure 14(a). Comparison between the total emissions given by the Ee, Oe and PV system for the different stages; (b). Emission balance
13 calculated for each stage, where a positive value is reported for the GHG in atmosphere, with negative values representative of the emissions
14 avoided thanks to the energy production provided by the contribution of the PV system.

15 4.7. *Limitations*

16 This study presents a number of limitations that have been divided into two parts: (i) limitations on solar
17 accessibility, land use in Norway and solar simulations and (ii) limitations on LCA procedure and calculation.
18 Firstly, it should be noted that the ZEB *Base Case* was originally designed as a generic concept model for the
19 local climatic conditions of Oslo (Norway), and the building was considered to be a detached house without any
20 urban surrounding. This is quite an important assumption, considering that the Norwegian national guidelines
21 [85] regulate the limitations of land use for the development plan of cities in Norway based on European
22 regulations [86]. Indeed, Norwegian municipalities are considering urban densification as a key issue for the
23 future. In this regard, one of the most relevant challenges in terms of planning for land management is to address
24 the anticipated future population growth. For example, some municipalities have planned a specific development
25 strategy to harmonize the design of the new districts with the city's current layout [87]. Therefore, municipal
26 guidelines for urban design and architecture [88] indicate that the main densification development strategy is for
27 a reduction in the number of detached houses and buildings that host only a small number of households. Data
28 regarding dwellings in Norway supports this trend by showing that, despite the majority of the population still
29 living in detached houses or in small buildings with four or fewer dwelling's, multi-dwelling buildings have seen
30 the largest rise in prevalence in recent years and they are filling out the existing voids in urban settlements [89].
31 Related to this aspect, it is relevant to underline that in relation to urban densification, significant impacts on the

orientation and exposure of the building's façades need to be taken into account, given their significant impacts on the variation of solar accessibility of the buildings and on the solar potential for the energy production from the solar systems installed on the buildings' envelope. In fact, the presence of other buildings in proximity to the analyzed one, may affect both the positions and geometry of the solar systems on the building envelope, as well as the available solar potential radiation due to overshadowing and/or solar reflections caused by the presence of the surrounding buildings. Previous studies have demonstrated that solar potential and PV localizations are significantly influenced by urban complexity and density [90, 91], as well as by the material finishes and colors of the façades [78, 80]. Another limitation linked to the solar energy relates to the energy production derived from the PV systems. In that regard, the calculation of the energy production in this study did not take into account the energy losses given by the PV system, electricity conversion losses in the inverter, in the grid, and due to the temperature at which the PV cells are operating. A paper by Good et al. [92], has demonstrated that combining modeling design tools (e.g. *Rhinoceros* and *Grasshopper*) with dynamic solar simulation software (*DIVA-for-Rhino*, *Radiance* etc.) and dedicated tools for energy outputs estimation (*PVsyst* and/or *Polysun*), results in a more complete and precise calculation of energy production from solar systems. In this way, all of the critical aspects from the overshadowing effect, solar reflection and the energy losses from the systems and the grid can be taken into account.

Secondly, in relation to the limitations of the LCA calculations, it has to be pointed out that they were conducted using mostly generic data reflecting European average production (from the *Ecoinvent* database) due to the limited availability of Norwegian EPD data at the time when this research was conducted. Since EPD data refers to specific building materials that are produced in Norway, the use of these better reflects the environmental impact of a building's location, such as Oslo, which was used in this study, and the Norwegian ultra-low-carbon energy mix, which has lower GHG emissions per kWh (40 gCO_2 per kWh in Norway compared to $\geq$ 500 gCO_2 per kWh in the rest of Europe [22, 71, 93]) of electricity compared to the significantly higher-carbon energy mix in the European grid. For this reason, the use of generic data limits the representativeness of the specific Norwegian conditions; however, at the same time, it allows for a wider comparison of the ZEB concept residential building at the European level. As shown in [46], the use of generic data instead of specific Norwegian EPDs generally overestimates the building's embodied GHG emissions, depending on the type of materials. In the case of the ZEB concept building, the use of generic data increases the total building embodied GHG emissions by a factor of 1.3.

Thirdly, the choice of the electricity-to-emissions conversion factor (132 gCO_2eq/kWh, ZEB factor) is particularly important, given that the ZEB residential concept is an all-electric building and it is calculated for a lifetime of 60 years in the future. In Georges et al. [27], the conversion factor for electricity was shown to significantly impact the overall GHG emission balance of the ZEB concept. By using a very-low-carbon energy mix (such as Norwegian internal electricity production), the avoided embodied emissions given by the PV system never balance the embodied emissions of the building components and the PV system. Thus, a zero emissions balance cannot be reached. Moreover, in such a scenario, the importance of the embodied GHG emissions increases, as those attributed to operational energy use alone are marginal [27, 94]. In such a perspective, the origin and the specific energy mix bounded in the building components acquire a critical importance in order to achieve a low life cycle impact of the ZEB concept.

Fourthly, in this study, the replacement phase of the building elements (phase B4) has been applied to the PV system only, in contrast to the *Base Case*, which additionally accounted for replacement emissions of the building materials, as described in [45, 46, 95]. This underestimates the life cycle GHG emissions, given that the environmental impact of repetitive substitution of materials has not been taken into account. Some finishing materials (such as external paint and plaster) and elements of the heating and ventilation systems are, in this regard, likely to increase the building life cycle impact, given their short service life [96, 97, 98]. According to Hoxha et al. [97], the relative contribution to the total building GHG emissions of those building components that undergo replacements, ranges from 5–10% for energy, sanitary, and electrical equipment, up to 10–20% for finishing, windows and doors.

Fifthly, The transportation to the building site (phase A4, as in Table 1) was not included in the calculation of the building's embodied GHG emissions; this is likely to increase when the solution with the autoclaved concrete blocks is used. One of the main disadvantages of this material, in terms of embodied emissions, derives from its production on site, given that it is mostly produced in Germany, with consideration to the emissions related to transport to the building site in Oslo. It should be noted that even though emissions from transport (A4) have not been included in this study, they have been included in the other studies in the ZEB centre and the IEA Annex 57 as described in [7, 55, 99, 100]. Mao et al. found that the impact of the transportation of materials and components to the building site accounts for 10% of the emissions for the production of those materials, given the use of diesel trucks and trains, for a distance up to 120 km from the production plants [101]. In such a perspective, given an average distance of 1,200 km between Oslo and a generic production plant in central Germany, the contribution of the phase A4 to the GHG emissions of the production phase (A1–A4 in Table 1) of autoclaved concrete blocks may likely increase by at least 10%.

Finally, the proposed workflow allows the shape of the building to be changed parametrically by multi-objective functions. This process allows the geometry and the quantity of materials in the building components to be automatically changed in real time. The same is not possible for the calculation of the operational energy. In fact, every time that the shape of the building has been optimized, the geometry needs to be exported from *Grasshopper* and imported into another computational environment in order to calculate the operational energy. Therefore, a further development of this study could involve the use of compatible software working on the *Grasshopper* platform, such as *Archsim* or *Ladybug* & *Honeybee*. However, because the latter software are currently under development, at this stage of the study, more established software such as *Design Builder*, with *EnergyPlus* as a computational engine, was selected.

5. **Conclusions**

This work presents an application of a generative algorithm in a workflow that has been applied on a ZEB *Base Case* located in Oslo in order to (i) conduct performance-based form-finding through multi-objective optimization and reduction of the quantity of the building's materials; and (ii) to perform energy and environmental analyses to enhance energy performance (solar radiation and daylighting) and to reduce the carbon footprint (embodied and operational emissions). The approach represents the development of an innovative and new methodology to apply parametric design principles to ZEB design by combining (i) generative modeling tools (*Rhinoceros* and *Grasshopper*) with (ii) evolutionary solvers (*Galapagos* and *Octopus)*, (iii) dynamic simulation analysis software (*Ladybug* and *DIVA-for-Grasshopper)*, and (iv) an LCA parametric algorithm (managed through the *Evaluate component* tool in *Grasshopper)*. This methodology

enables an iterative analysis by dynamically linking each parameter (e.g. geometry, size and position of openings, indoor visual comfort, material dimensions and quantities) and simultaneously investigating and comparing numerous building layouts and volumes. The method enables the real-time visualization of the impact resulting from each geometrical variation in the building design on both the embodied emissions of materials and the operational energy, both early on and throughout the design process. More specifically, the application of the methodology allowed the generation of a group of energy and environmentally responsive optimized shapes for the defined climate conditions (Oslo, Norway in this study). The ten best shapes were then selected as being the most suitable to exploit the solar potential at high latitudes. The building envelopes were optimized by harvesting vertical surfaces (up to 60° from the horizontal). This aspect underlines that the developed workflow would be able to deliver results particular to the climate of the geographical location in which the case study is located. In this respect, this approach provides the designer with a valuable and integrated assessment methodology that can be embedded in a holistic design approach. Furthermore, the approach has been developed to be replicable in different worldwide climatic contexts in order to support designers, architects and engineers when dealing with different architectural, aesthetic, and environmental challenges simultaneously and dynamically during each stage of the whole design process.

Acknowledgments

1 References

2

[1] IPCC, "Climate Change 2014: synthesis report", Contribution of Working Groups I, II and III to the Fifth Assessment Report of the Intergovernmental Panel on Climate Change. IPCC, 2014.

[2] *EPBD Directive 2010/31/EU of the European Parliament and of the Council of 19 May 2010 on the energy performance of buildings. European Commission,* 2010.

[3] *ASHRAE. Energy Standard for Buildings Except Low-Rise Residential Buildings, American Society of Heating, Refrigerating, and Air-Conditioning Engineers (ASHRAE) Standards Committee 90.1,* 2013.

[4] U. Berardi, "A cross-country comparison of the building energy consumptions and their trends", *Resources, Conservation and Recycling,* vol. 123, pp. 230–241, 2017.

[5] H. Birgisdottir, A. Moncaster, A. Houlihan Wiberg, C. Chae, K. K. Yokoyama, M. Balouktsi, S. Seo, T. Oka, T. Lützkendorf and T. Malmqvist, "IEA EBC Annex 57. Evaluation of Embodied Energy and CO2eq for Building Construction", *Energy and Buildings,* vol. 154, no. Supplement C, pp. 72–80, 2017.

[6] T. Oka, S. Seo, J. Zelezna, P. Hájek, H. Birgisdottir, F. Nygaard Rasmussen, A. Passer, T. Lützkendorf, M. Balouktsi, K. Yokoyama, C. Chae, T. Malmqvist, A. Houlihan Wiberg, M. Mistretta, A. Moncaster and N. Yokoo, "Evaluation of Embodied Energy and CO2eq for Building Construction (Annex 57)", International Energy Agency - Energy in Buildings and Communities Programme - Institute for Building Environment and Energy Conservation ISBN 978-4-909107-11-4, Tokyo, 2016.

[7] H. Birgisdottir, A. A. M. Houlihan Wiberg, T. Malmqvist, A. Moncaster and F. Nygaard Rasmussen, "International Energy Agency Evaluation of Embodied Energy and CO2eq for Building Construction (Annex 57) Subtask 4: Case studies and recommendations for the reduction of embodied energy and embodied greenhouse gas emissions from buildings", International Energy Agency, Institute for Building Environment and Energy Conservation, ISBN 978-4-909107-08-4, Japan, 2017.

[8] *ISO 21929-1:2011 Sustainability in building construction - Sustainability indicators - Part 1: Framework for the development of indicators and a core set of indicators for buildings,* 2011.

[9] *ISO 21931-1:2010 Sustainability in building construction - Framework for methods of assessment of the environmental performance of construction works - Part 1: Buildings,* 2010.

[10] *EN 15643-2:2011 Sustainability of construction works. Assessment of buildings. Framework for the assessment of environmental performance,* 2011.

[11] *EN 15978:2011 - Sustainability of construction works. Assessment of environmental performance of buildings. Calculation method,* 2011.

[12] *Communication from the commission to the European parliament, the council, the European economic and social committee and the committeee of the regions - Energy Roadmap 2050,* 2011.

[13] S. Pless and P. Torcellini, "Net-zero energy buildings: A classification system based on renewable energy supply options", Technical Report NREL/TP-550-44586, Golden, Colorado: NREL, June 2010.

[14] P. Torcellini, S. Pless, M. Deru and D. Crawley, "Zero Energy Buildings: A Critical Look at the Definition", National Renewable Energy Laboratory and Department of Energy, US, 2006.

[15] U. Berardi, "ZEB and NZEB (definitions, design methodologies, good practices and case studies)", in *Handbook of Energy Efficiency in Buildings*, Elsevier (ed. U. Desideri and F. Asdrubali), 2018, pp. 81-111.

[16] F. Garde and M. Donn, *Solution Sets and Net Zero Energy Buildings: A review of 30 Net ZEBs case studies worldwide*, Le Tampon, Reunion, 2014.

[17] K. Voss and E. Musall, *Net zero energy buildings*, Detail, 2012.

[18] F. Garde, J. Ayoub, D. Aelenei, L. Aelenei and A. Scognamiglio, *Solution Sets for Net-Zero Energy Buildings*, Berlin, Germany: Ernst & Sohn, 2017.

[19] J. Cho, S. Shin, J. Kim and H. Hong, "Development of an energy evaluation methodology to make multiple predictions of the HVAC&R system energy demand for office buildings," *Energy and Buildings ,* no. 80 , p. 169–183, 2014.

[20] A. O. W. Athienitis, Modeling, Design, and Optimization of Net-Zero Energy Buildings, Wiley, 2015.

[21] A. J. Marszal, P. Heiselberg, J. S. Bourrelle, E. Musall, K. Voss, I. Sartori and A. Napolitano, "Zero Energy Building – A review of definitions and calculation methodologies," *Energy and Buildings,* vol. 43, no. 4, p. 971–979, 2011.

[22] I. Sartori, A. Napolitano and K. Voss, "Net zero energy buildings: A consistent definition framework," *Energy and Buildings,* vol. 48, pp. 220-232, 2012.

[23] M. Cellura, F. Guarino, S. Longo and M. Mistretta, "Energy life-cycle approach in Net zero energy buildings balance: Operation and embodied energy of an Italian case study", *Energy and Buildings,* vol. 72, pp. 371–381, 2014.

[24] P. Hernandez and P. Kenny, "From net energy to zero energy buildings: Defining life cycle zero energy buildings", *Energy and Buildings,* vol. 42, pp. 815–821, 2010.

[25] H. Lund, A. Marszal and P. Heiselberg, "Zero energy buildings and mismatch compensation factors," *Energy and Buildings,* no. 43 (7), pp. 1646–1654, 2011.

[26] *ISO 14040:2006 - Environmental management - Life cycle assessment - Principles and framework,* 2006.

[27] L. Georges, M. Haase, A. Houlihan Wiberg, T. Kristjansdottir and B. Risholt, "Life cycle emissions analysis of two nZEB concepts", *Building Research and Information,* vol. 43, no. 1, pp. 82–93, 2015.

[28] K. Adalberth, "Energy use during the life cycle of buildings: a method", *Building and Environment,* vol. 32, no. 4, pp. 317–320, 1997.

[29] K. Adalberth, "Energy use during the life cycle of single-unit dwellings: Examples", *Building and Environment,* vol. 32, no. 4, pp. 321–329, 1997.

[30] L. Gustavsson, A. Joelsson and R. Sathre, "Life cycle primary energy use and carbon emission of an eight-storey wood-framed apartment building", *Energy and Buildings,* no. 42 (2), pp. 230–242, 2010.

[31] C. Thiel, "A Material Life Cycle Assessment of a Net-Zero Energy Building," *Energies,* no. 6 (2), p. 1125, 2013.

[32] F. Pomponi, P. Piroozfar, R. Southall, P. Ashton and E. Farr, "Life cycle energy and carbon assessment of double skin façades for office refurbishments", *Energy and Buildings,* vol. 109, pp. 143–156, 2015.

[33] N. Lolli and I. Andresen, "Aerogel vs. argon insulation in windows: A greenhouse gas emissions analysis", *Building and Environment,* vol. 101, pp. 64–76, 2016.

[34] A. Säynäjoki, J. Heinonen, S. Junnila and A. Horvath, "Can life-cycle assessment produce reliable policy guidelines in the building sector?" *Environ. Res. Lett.,* vol. 12, pp. 1–16, 2017.

[35] C. Anand and M. Amor, "Recent developments, future challenges and new research directions in LCA of buildings: A critical review", *Renewable and Sustainable Energy Reviews,* vol. 67, no. C, pp. 408–416, 2017.

[36] L. V. Rasmussen, R. Bierbaum, J. A. Oldekop and A. Agrawal, "Bridging the practitioner-researcher dividIndicators to track environmental, economic, and sociocultural sustainability of agricultural commodity production", *Global Environmental Change,* vol. 42, pp. 33–46, 2017.

[37] F. Pomponi and A. Moncaster, "Embodied carbon mitigation and reduction in the built environment – What does the evidence say?" *Journal of Environmental Management,* vol. 181, pp. 687–700, 2016.

[38] T. Lützkendorf, G. Foliente, M. Balouktsi and A. Houlihan Wiberg, "Net-zero buildings: Incorporating embodied impacts", *Building Research and Information,* vol. 43, no. 1, pp. 62–81, 2015.

[39] A. Moncaster and J. Song, "A comparative review of existing data andmethodologies for calculating embodied energy and carbon of buildings", *Int. J.Sustainable Build. Technol. Urban Dev.,* vol. 3, no. 1, pp. 26–36, 2012.

[40] *NS3700:2013 Criteria for passive houses and low energy buildings - Residential buildings,* 2013.

[41] *NS3701:2012 Criteria for passive houses and low energy buildings - Non-residential buildings,* 2012.

[42] T. H. Dokka, I. Sartori, M. Thyolt, K. Lien and K. B. Lindeberg, "A Norwegian zero emission building definition", in *Passihus Norden 2013*, Götheborg, Sweden, 2013.

[43] T. Kristjansdottir, H. Fjeldheim, E. Selvig, B. Risholt, B. Time, L. Georges, T. H. Dokka, J. Bourelle, R. Bohne and Z. Cervenka, *A Norwegian ZEB Definition - Embodied Emissions*, ZEB Project report no. 17, SINTEF Academic Press, Trondheim, ISBN 978-82-536-1398-7, Norway, 2014.

[44] S. M. Fufa, R. D. Schlanbusch, K. Sornes, M. Inman and I. Andresen, *A Norwegian ZEB definition guideline*. ZEB Project report no. 29, SINTEF Academic Press, Trondheim, ISBN 978-82-536-1513-4, Norway, 2016.

[45] T. H. Dokka, A. Houlihan Wiberg, L. Georges, S. Mellegård, B. Time, M. Haase, M. Maltha and A. G. Lien, *A zero emission concept analysis of an office building,* ZEB Project report no. 9, The Research Centre on Zero Emission Building, ISBN 978-82-536-1324-6, Trondheim, 2013.

[46] A. Houlihan Wiberg, L. Georges, S.-M. Fufa, B. Risholt and C. Good, *A zero emission concept analysis: Part 2 sensitivity analysis*. ZEB Project report no. 21, The Research Centre on Zero Emission Buildings, ISBN 978-82-536-1449, Trondheim, 2015.

[47] A. Houlihan Wiberg, L. Georges, T. H. Dokka, M. Haase, B. Time, A. G. Lien, S. Mellegård and M. Maltha, "A net zero emission concept analysis of a single-family house", *Energy and Buildings,* vol. 74, no. Supplement C, pp. 101–110, 2014.

[48] R. Aish, *Introduction to Generative Components: A parametric and associative design system for architecture, building engineering and digital fabrication,* Bentley Systems, 2005.

[49] R. Evins, "A review of computational optimisation methods applied to sustainable building design", *Renewable and Sustainable Energy Reviews,* no. 22, pp. 230–245, 2013.

[50] Y. Yun Kyu and A. M. Malkawi, "Optimizing building form for energy performance based on hierarchical geometry relation," *Automation in Construction,* no. 18, pp. 825–833, 2009.

[51] G. Lobaccaro, S. Chatzichristos and A. Viridiana, "Solar Optimization of Housing Development", *Energy Procedia,* vol. 91, pp. 868–875, 2016.

[52] A. Zani, L. C. Tagliabue, T. Poli, A. L. C. Ciribini, E. De Angelis and M. Manfren, "Occupancy profile variation analyzed through generative modelling to control building energy behavior", *Procedia Engineering,* no. 180, pp. 1495–1505, 2017.

[53] N. Lolli, S. M. Fufa and M. Inman, "A parametric tool for the assessment of operational energy use, embodied energy and embodied material emissions in building", *Energy Procedia,* no. 111, pp. 21–30, 2017.

[54] Z. Tuncer and A. Houlihan Wiberg, "ZEB Tool - Transition to an Integrated and Dynamic Dashboard", Masters theory report submitted in June 2017. Norwegian University of Science & Technology, Trondheim, Unpublished results.

[55] M. Slånke, H. Auckland, A. Houlihan Wiberg and E. Reisch, "Visual LCA in ZENs. Interactive visualisation network for material associated GHG in preliminary neighbourhood design stages", Masters thesis submitted June 2017. Norwegian University of Science & Technology, Trondheim, Unpublished results.

[56] A. Kokkos, "Design for Deconstruction plugin for Grasshopper," 2015. [Online]. Available: http://www.grasshopper3d.com/video/design-for-deconstruction-plugin-for-grasshopper. [Accessed 1 April 2016].

[57] A. Hollberg and J. Ruth, "LCA in architectural design—a parametric approach", *The International Journal of Life Cycle Assessment,* vol. 21, no. 7, pp. 943–960, 2016.

[58] A. Azzouz, M. Borchers, J. Moreira and A. Mavrogianni, " Life cycle assessment of energy conservation measures during early stage office building design: A case study in London, UK", *Energy and Buildings,* vol. 139, pp. 547–568, 2017.

[59] P. Ylmén, K. Mjörnell, J. Berlin and J. Arfvidsson, "The influence of secondary effects on global warming and cost optimization of insulation in the building envelope", *Building and Environment,* vol. 118, pp. 174–183, 2017.

[60] H. Ramin, P. Hanafizadeh, T. Ehterami and M. Ali AkhavanBehabadi, "Life cycle-based multi-objective optimization of wall structures in climate of Tehran," *Advances in Building Energy Research,* pp. 1-14, 2017.

[61] M. Braulio-Gonzalo and M. D. Bovea, "Environmental and cost performance of building's envelope insulation materials to reduce energy demand: Thickness optimisation", *Energy and Buildings,* vol. 150, pp. 527–545, 2017.

[62] F. Pomponi and B. D'Amico, "Holistic study of a timber double skin façade: Whole life carbon emissions and structural optimisation", *Building and Environment,* vol. 124, pp. 42–56, 2017.

[63] P. Bonomo, F. Frontini, P. De Berardinis and I. Donsante, "BIPV: building envelope solutions in a multi-criteria approach. A method for assessing life-cycle costs in the early design phase", *Advances in Building Energy Research,* vol. 11, no. 1, pp. 104–129, 2017.

[64] M. Ashouri, F. Razi Astaraei, R. Ghasempour, M. H. Ahmadi and M. Feidt, "Optimum insulation thickness determination of a building wall using exergetic life cycle assessment", *Applied Thermal Engineering,* vol. 106, pp. 307–315, 2016.

[65] R. Azari, S. Garshasbi, P. Amini, H. Rashed-Ali and Y. Mohammadi, "Multi-objective optimization of building envelope design for life cycle environmental performance", *Energy and Buildings,* vol. 126, pp. 524–534, 2016.

[66] L. Caldas, *An evaluation based generative design system: using adaptation to shape architectural form*, MIT Press, 2001.

[67] S. Davidson, "Grasshopper: Algorithmic Modelling for Rhino, NING/MODE", 2013. [Online]. Available: http://www.grasshopper3d.com/. [Accessed 11 April 2017].

[68] *NS 3940:2012 Calculation of areas and volumes of buildings,* 2012.

[69] McNeel Robert and Associates, "Rhinoceros Version 5.0", 2015.

[70] US Department of Energy, "Weather Data", EnergyPlus U.S. Department of Energy's (DOE) Building Technologies Office (BTO), the National Renewable Energy Laboratory (NREL), 2016. [Online]. Available: https://energyplus.net/weather. [Accessed 15 May 2016].

[71] I. Graabak, B. H. Bakken and N. Feilberg, "Zero Emission Building and Conversion Factors between Electricity Consumption and Emissions of Greenhouse Gases in a Long Term Perspective", *Environmental and Climate Technologies,* vol. 13, no. 1, pp. 12–19, 2013.

[72] M. Sadeghipour Roudsari, "Ladybug Tools", [Online]. Available: http://www.grasshopper3d.com/group/ladybug. [Accessed 11 February 2015].

[73] Jared Tarbell, algorithm: "Substrate", 2003. [Online]. Available: http://www.complexification.net/gallery/machines/substrate/index.php. [Accessed 21 March 2015].

[74] A. McNeil and E. S. Lee, "A validation of the Radiance three-phase simulation method for modelling annual daylight performance of optically complex fenestration systems", *Journal of Building Performance Simulation,* vol. 6, pp. 24–37, 2013.

[75] J. Mardaljevic, "Simulation of annual daylighting profiles for internal illuminance", *Lighting Research & Technology,* vol. 32, no. 3, pp. 111–118, 2000.

[76] A. J. Jakubiec and C. F. Reinhart, "DIVA 2.0: Integrating daylight and thermal simulations using Rhinoceros 3D, Daysim and EnergyPlus", in *Proceedings of Building Simulation: 12th Conference of International Building Performance Simulation Association*, Sydney, 2001.

[77] U. Berardi and T. Wang, "Daylighting in an atrium-type high performance house", *Building and Environment,* vol. 76, pp. 92–104, 2014.

[78] G. Lobaccaro, F. Fiorito, G. Masera and T. Poli, "District Geometry Simulation: A Study for the Optimization of Solar Façades in Urban Canopy Layers", *Energy Procedia,* vol. 30, pp. 1163–1172, 2012.

[79] C. F. Reinhart and J. Wienold, "The daylighting dashboard – A simulation-based design analysis for daylit spaces", *Building and Environment,* vol. 46, no. 2, pp. 386–396, 2011.

[80] G. Lobaccaro, S. Carlucci, S. Croce, R. Paparella and L. Finocchiaro, "Boosting solar accessibility and potential of urban districts in the Nordic climate: A case study in Trondheim", *Solar Energy,* vol. 149, pp. 347–369, 2017.

[81] D. Chwieduk and B. Bogdanska, "Some recommendations for inclinations and orientations of building elements under

solar radiation in Polish conditions", *Renewable Energy,* vol. 29, pp. 1569–1581, 2004.

[82] R. Compagnon, "Solar and daylight availability in the urban fabric", *Energy and Buildings,* vol. 36, pp. 321–328, 2004.

[83] G. Y. Yun and K. Steemers, "Implications of urban settings for the design of photovoltaic and conventional facades", *Solar Energy,* vol. 83, pp. 69–80, 2009.

[84] Revolvy, LLC, "Daylight factor", 2014. [Online]. Available: https://www.revolvy.com/topic/Daylight%20factor&item_type=topic. [Accessed 15 January 2015].

[85] Kommunal- og moderniseringsdepartementet, "Nasjonale forventninger til regional og kommunal planlegging (National expectations regarding regional and municipal planning)", Royal Resolution, 2015.

[86] European Commission, *Guidelines on best practice to limit, mitigate or compensate soil sealing,* Brussels, 2012.

[87] Trondheim Kommune, "Kommuneplanens arealdel 2012 - 2024 (Municipal masterplan)", Trondheim Kommune, Trondheim, 2012.

[88] Bygningsrådet, "Veileder for byform og arkitektur (Guidelines for urban design and architecture)", Trondheim Kommune, Trondheim, 2013.

[89] Statistisk sentralbyrå - Statistics Norway, "Dwellings (occupied and vacant), by buildingtype and year - Dwellings, 1 January 2016", Statistisk sentralbyrå - Statistics Norway, 21 June 2016. [Online]. Available: https://www.ssb.no/en/bygg-bolig-og-eiendom/statistikker/boligstat. [Accessed 30 June 2016].

[90] E. Nault, G. Peronato, E. Rey and M. Andersen, "Review and critical analysis of early-design phase evaluation metrics for the solar potential of neighborhood designs", *Building and Environment,* vol. 92, pp. 679–691, 2015.

[91] J. Kanters and M. Wall, "A planning process map for solar buildings in urban environments", *Renewable and Sustainable Energy Reviews,* vol. 57, pp. 173–185, 2016.

[92] C. S. Good, G. Lobaccaro and S. Hårklau, "Optimization of Solar Energy Potential for Buildings in Urban Areas – A Norwegian Case Study", *Energy Procedia,* vol. 58, pp. 166–171, 2014.

[93] F. Noris, E. Musall, J. Salom, B. Berggren, S. Ø. Jensen, K. B. Lindeberg and I. Sartori, "Implications of weighting factors on technology preference in net zero energy buildings", *Energy and Buildings,* vol. 82, pp. 250–262, 2014.

[94] N. Lolli and A. G. Hestnes, "The influence of different electricity-to-emissions conversion factors on the choice of insulation materials", *Energy and Buildings,* vol. 85, pp. 362–373, 2014.

[95] T. F. Kristjansdottir, N. Heeren, I. Andresen and H. Brattebø, "Comparative emission analysis of low-energy and zero-emission buildings", *Building Research & Information,* pp. 1–16, 2017.

[96] I. Blom, L. Itard and A. Meijer, "Environmental impact of dwellings in use: Maintenance of façade components", *Building and Environment,* vol. 45, no. 11, pp. 2526–2538, 2010.

[97] E. Hoxha, G. Habert, S. Lasvaux, J. Chevalier and R. Le Roy, "Influence of construction material uncertainties on residential building LCA reliability", *Journal of Cleaner Production,* vol. 144, pp. 33–47, 2017.

[98] X. Oregi, P. Hernandez and R. Hernandez, "Analysis of life-cycle boundaries for environmental and economic assessment of building energy refurbishment projects", *Energy and Buildings,* vol. 136, pp. 12–25, 2017.

[99] K. Yokoyama, H. Birgisdottir, T. Malmqvist, A. Houlihan Wiberg, A. Moncaster, S. Seo, A. Passer, T. Lützkendorf, M. Balouktsi, F. Nygaard Rasmussen, M. Mistretta, T. Oka, C.-U. Chae, R. Frischknecht, N. Yokoo, P. Hájek and J. Zelezna, *International Energy Agency Evaluation of Embodied Energy and CO2eq for Building Construction (Annex 57) Overview of Annex 57 Results*, ISBN 978-4-909107-10-7, 2017.

[100] M. R. K. Wiik and A. A. M. Houlihan Wiberg, "Life Cycle Greenhouse Gas Emissions of Material Use in the Living Laboratory", in *Proceedings of World Sustainable Built Environment Conference 2017 Hong Kong. Transforming Our Built Environment through Innovation and Integration: Putting Ideas into Action WSBE17*, Hong Kong, 2017.

[101] C. Mao, Q. Shen, L. Shen and L. Tang, "Comparative study of greenhouse gas emissions between off-site prefabrication and conventional construction methods: Two case studies of residential projects", *Energy and Buildings,* vol. 66, pp. 165–176, 2013.

1

2